

MDPI

Article

A Particle Swarm Optimization-Guided Ivy Algorithm for Global Optimization Problems

Kaifan Zhang ¹, Fujiang Yuan ^{2,*}, Yang Jiang ³, Zebing Mao ⁴, Zihao Zuo ³ and Yanhong Peng ^{3,5,*}

- School of Computer Science, Hubei University of Technology, Wuhan 430068, China
- School of Computer Science and Technology, Taiyuan Normal University, Taiyuan 030619, China
- ³ College of Mechanical Engineering, Chongqing University of Technology, Chongqing 400054, China
- Department of Engineering Science and Mechanics, Shibaura Institute of Technology, 3-7-5 Toyosu, Koto-ku, Tokyo 135-8548, Japan
- Chongqing Institute of Green and Intelligent Technology, Chinese Academy of Sciences, Chongqing 400714, China
- * Correspondence: yuanfujiang@ctbu.edu.cn (F.Y.); yhpeng@nagoya-u.jp (Y.P.)

Abstract: In recent years, metaheuristic algorithms have garnered significant attention for their efficiency in solving complex optimization problems. However, their performance critically depends on maintaining a balance between global exploration and local exploitation; a deficiency in either can result in premature convergence to local optima or low convergence efficiency. To address this challenge, this paper proposes an enhanced ivy algorithm guided by a particle swarm optimization (PSO) mechanism, referred to as IVYPSO. This hybrid approach integrates PSO's velocity update strategy for global searches with the ivy algorithm's growth strategy for local exploitation and introduces an ivy-inspired variable to intensify random perturbations. These enhancements collectively improve the algorithm's ability to escape local optima and enhance the search stability. Furthermore, IVYPSO adaptively selects between local growth and global diffusion strategies based on the fitness difference between the current solution and the global best, thereby improving the solution diversity and convergence accuracy. To assess the effectiveness of IVYPSO, comprehensive experiments were conducted on 26 standard benchmark functions and three real-world engineering optimization problems, with the performance compared against 11 state-of-the-art intelligent optimization algorithms. The results demonstrate that IVYPSO outperformed most competing algorithms on the majority of benchmark functions, exhibiting superior search capability and robustness. In the stability analysis, IVYPSO consistently achieved the global optimum across multiple runs on the three engineering cases with reduced computational time, attaining a 100% success rate (SR), which highlights its strong global optimization ability and excellent repeatability.

Keywords: particle swarm optimization; ivy algorithm; global optimization ability



Academic Editor: Heming Jia

Received: 21 April 2025 Revised: 16 May 2025 Accepted: 17 May 2025 Published: 21 May 2025

Citation: Zhang, K.; Yuan, F.; Jiang, Y.; Mao, Z.; Zuo, Z.; Peng, Y. A Particle Swarm Optimization-Guided Ivy Algorithm for Global Optimization Problems. *Biomimetics* **2025**, *10*, 342. https://doi.org/10.3390/biomimetics10050342

Copyright: © 2025 by the authors. Licensee MDPI, Basel, Switzerland. This article is an open access article distributed under the terms and conditions of the Creative Commons Attribution (CC BY) license (https://creativecommons.org/licenses/by/4.0/).

1. Introduction

Metaheuristic algorithms have become vital tools for addressing complex optimization problems and are widely applied in fields such as engineering design [1,2], machine learning [3,4], and control systems [5,6]. Compared to traditional mathematical optimization techniques, such as gradient-based techniques [7], metaheuristics offer several advantages; they do not require gradient information, exhibit low sensitivity to initial conditions, and are well-suited for high-dimensional or multimodal problems [8,9]. Their flexibility in navigating the solution space and capability to avoid entrapment in local optima have made them a central focus in computational intelligence research [10,11].

In recent years, hybridization techniques have been increasingly employed to enhance the performance of metaheuristics by integrating complementary strategies from different algorithms, thereby improving the convergence speed, solution quality, and robustness [12–15]. Among these, particle swarm optimization (PSO) has received considerable attention due to its simplicity and rapid convergence [16]. However, PSO also suffers from limited local exploitation ability and a tendency toward premature convergence. To mitigate these issues, numerous studies have combined particle swarm optimization (PSO) with evolutionary operators such as genetic algorithms (GA) [17] and differential evolution (DE) [18], adaptive parameter control techniques [19], and multi-strategy perturbation schemes to better balance global exploration and local exploitation [20].

In parallel, the ivy algorithm (IVYA) has emerged as a promising bio-inspired approach due to its straightforward design and strong local search capabilities [21]. By mimicking the natural growth and propagation behaviors of ivy plants, IVYA can efficiently exploit the neighborhood of promising regions while preserving population diversity. Nevertheless, the lack of a global guidance mechanism limits its convergence efficiency on large-scale optimization problems.

Despite the development of various hybrid metaheuristics, most existing methods primarily focus on accelerating convergence or maintaining diversity, without effectively addressing how to preserve the exploration–exploitation balance while avoiding premature convergence. Moreover, mechanisms that adaptively adjust search strategies based on dynamic fitness landscapes remain underexplored in the current literature.

To bridge these gaps, this paper introduces a novel hybrid optimization algorithm—IVYPSO—which synergistically combines the global guidance of PSO with the adaptive local search capabilities of IVYA. IVYPSO incorporates a biologically inspired ivy perturbation variable (GV) into the PSO velocity update equation, enabling adaptive directional control and stochastic perturbations based on the current fitness landscape. This design enhances the algorithm's ability to escape local optima while improving the population diversity and convergence stability. The main contributions of this work are summarized as follows:

- A novel PSO-guided hybrid optimization algorithm, IVYPSO, is proposed. It embeds
 the ivy growth strategy of IVYA into the velocity update process of PSO, thereby
 enabling dynamic switching between local and global search modes.
- A balanced search framework was constructed by comparing the fitness of the current individual with that of the global best. The algorithm dynamically determines whether to perform local exploitation or global exploration, thereby improving its adaptability to complex search spaces.
- 3. A comprehensive experimental evaluation was conducted on 26 standard benchmark functions and three constrained real-world engineering design problems. The performance of the proposed IVYPSO algorithm was compared against eleven advanced metaheuristic optimization algorithms, including classical methods (such as PSO, IVY, BOA, WOA, and GOOSE), as well as recently developed hybrid algorithms from high-quality research studies (including HPSOBOA, FDC-AGDE, dFDB-LSHADE, NSM-BO, dFDB-SFS, and FDB-AGSK). The experimental results demonstrate that IVYPSO consistently outperformed the compared algorithms in terms of optimization accuracy, convergence speed, and robustness.

The rest of this paper is organized as follows. Section 2 reviews the related work concerning the design and development of metaheuristic search algorithms. Section 3 introduces the PSO and ivy algorithms. Section 4 presents the proposed IVYPSO hybrid algorithm. Section 5 covers its testing on benchmark functions and applications for practical engineering problems. Section 6 discusses the results and outlines future work.

Biomimetics 2025, 10, 342 3 of 41

2. Related Work

Metaheuristic algorithms have become essential tools for addressing complex, multimodal, and high-dimensional optimization problems. Inspired by natural, biological, or social phenomena, these gradient-free algorithms are particularly well-suited for real-world engineering applications. Recent advancements in metaheuristics have shifted the research focus toward enhancing the algorithmic performance by redesigning key components namely, the guiding mechanisms, convergence strategies, and update schemes.

Among these components, the guiding mechanism is critical, as it governs how individuals or candidate solutions are influenced by others within the population. Traditional guidance approaches, such as those used in classical PSO, typically direct individuals toward global or local optima based on fitness values but often suffer from premature convergence and loss of population diversity. To address these challenges, advanced guiding strategies have been developed, including fitness distance balance (FDB) [22], adaptive FDB (AFDB) [23], dynamic FDB (DFDB) [24], and fitness distance constraint (FDC). By incorporating spatial distance information between solutions, these methods achieve a more balanced trade-off between exploration and exploitation, as demonstrated by their successful integration into algorithms such as FDC_AGDE [25], dFDB_LSHADE [26], dFDB_SFS [27], and FDB_AGSK [28], which exhibit strong performance on benchmark functions and engineering problems.

Convergence strategies, which determine how candidate solutions are updated each iteration, also play a pivotal role in directing search trajectories and influencing the convergence speed. The contemporary approaches include time-decreasing control parameters, multi-phase convergence schemes, and hybrid deterministic random update models. For instance, the GOOSE algorithm adapts its convergence behavior across different search stages [29], while HPSOBOA incorporates multiple convergence modes to sustain robustness across diverse problem domains [30].

Moreover, update schemes—particularly for the selection of surviving individuals—are vital for maintaining the solution quality and population diversity. Conventional methods relying solely on fitness-based ranking risk stagnation and premature convergence. To overcome this, the natural survivor method (NSM) integrates the fitness performance with historical success rates to judiciously select individuals for the next generation [31]. NSM has proven effective in algorithms such as NSM-BO and NSM-LSHADE-CnEpSin [32], markedly enhancing the stability and global search performance in constrained engineering problems.

Despite these advances, most existing studies focus on improving individual algorithmic components—such as the convergence behavior or update strategies—often at the expense of overall adaptability or diversity. A unified framework that simultaneously integrates global guidance and bio-inspired local searches with dynamic adaptability remains lacking.

To bridge this gap, we propose a hybrid algorithm, IVYPSO, which synergistically combines PSO's global search capability with the ivy algorithm's local growth and diffusion mechanisms. By embedding a dynamic ivy-inspired variable GV within the PSO velocity update formula, IVYPSO adaptively switches search strategies based on individual fitness, effectively balancing exploration and exploitation. This design not only preserves the convergence accuracy but also enhances the robustness and diversity, offering a novel high-performance optimization framework tailored for complex global optimization challenges.

3. Materials and Methods

To better illustrate our hybrid algorithm, the inspiration behind and detailed implementation of the PSO algorithm and ivy algorithm will be introduced.

Biomimetics **2025**, 10, 342 4 of 41

3.1. PSO Formulation

PSO is a nature-inspired swarm intelligence algorithm, proposed by Kennedy and Eberhart in 1995. Its core idea is based on simulating the foraging behavior of bird flocks or fish schools. By sharing information and collaborating among individuals, PSO strikes a balance between global exploration and local exploitation, effectively solving optimization problems.

In the PSO algorithm, each particle has a unique position $X_i = [x_{i1}, x_{i2}, x_{i3}, \dots, x_{ij}, \dots, x_{iD}]$ and velocity $V_i = [v_{i1}, v_{i2}, v_{i3}, \dots, v_{ij}, \dots, v_{iD}]$, representing a potential solution. Here, $j = 1, 2, \dots, D$, D denotes the dimensionality of the search space. In each iteration, the position of the particle is dynamically updated based on the following three components:

- (1) Inertia component: Determined by the particle's previous velocity, it is used to maintain the particle's movement trend and balance the global exploration capability of the search.
- (2) Individual cognitive component: The particle adjusts its search direction based on its own historical best position P_{best} , simulating individual learning behavior.
- (3) Social component: The particle adjusts its direction based on the entire population's global best position G_{best} , reflecting social learning and collaborative effects.

During the search process, the particle's position is influenced by its best position in the neighborhood $P_{best,i}$ and the global best position G_{best} of the entire population.

The particle position and velocity update formulas are given by Equations (1) and (2), respectively:

$$X_{i}^{k+1} = X_{i}^{k} + V_{i}^{k+1} \tag{1}$$

$$V_{i}^{k+1} = wV_{i}^{k} + c_{1}r_{1}\left(P_{\text{best},i} - X_{i}^{k}\right) + c_{2}r_{2}\left(G_{\text{best}} - X_{i}^{k}\right)$$
(2)

where w is the inertia weight, which controls the balance between global and local searches; c_1 and c_2 are acceleration coefficients that determine the influence of individual and group learning, respectively; c_1r_1 and c_2r_2 are random numbers, ranging from 0 to 1, which enhance the randomness of the search.

The flowchart of the PSO algorithm is shown in Figure 1.

3.2. IVYA Formulation

The ivy algorithm, derived from the growth behavior of ivy plants in nature, is a swarm intelligence optimization method. Ivy plants continuously grow, climb, and spread in the environment in search of sunlight, nutrients, and other resources for survival. This process serves as inspiration for addressing global optimization problems. The algorithm simulates the different life stages of ivy, including growth, ascent, and spreading [33]. The algorithm's implementation process can be outlined in the subsequent four steps:

(1) Initialize the population, where N and D represent the total number of members and the dimensionality of the problem, respectively. Thus, the i-th population member has the form $I_i=(I_{i1},\ldots,I_{iD})$, where $i=1,2,\ldots,N$, The total population of ivy plants is represented as $\overrightarrow{I}=(I_1,\ldots,I_i,\ldots,I_{Npop})$, At the start of the algorithm, the initial positions of the ivy algorithm population in the search space are determined using Equation (3):

$$I_{i} = I_{min} + rand(1, D) \odot (I_{max} - I_{min}), i = 1, ..., N$$
 (3)

where rand(1, D) represents a vector of dimension D with random numbers uniformly distributed in the range [0, 1]. The upper and lower limits of the search space are

Biomimetics **2025**, 10, 342 5 of 41

denoted by I_{max} and I_{min} , respectively, and \odot denotes the element-wise product of two vectors.

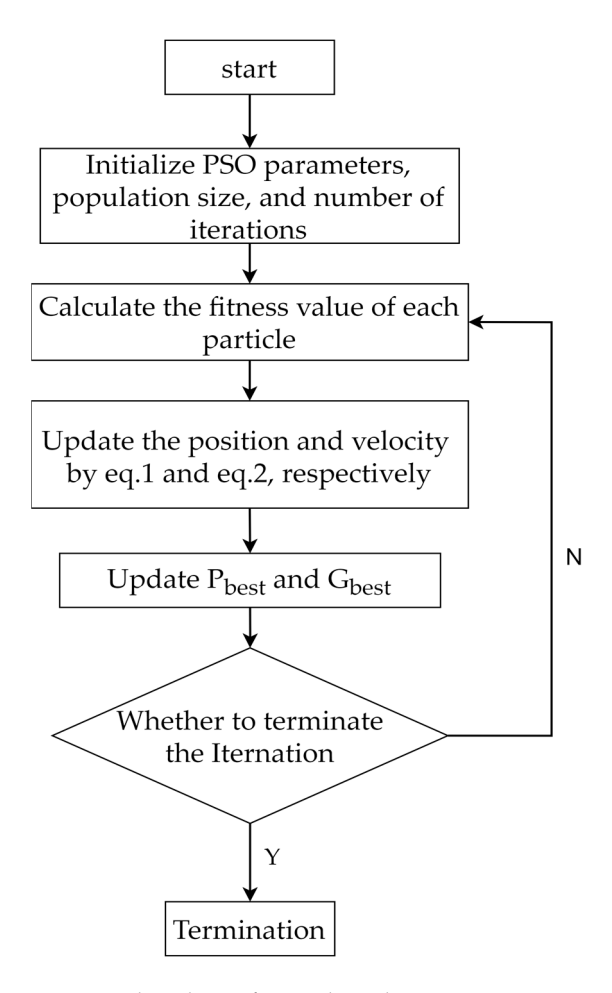


Figure 1. Flowchart of PSO algorithm.

(2) Coordinated and disciplined population growth. In the growth process of the ivy algorithm, we assume that the growth rate GV of the ivy algorithm is a function of time, expressed through a differential equation, as illustrated in Equation (4):

$$\frac{dGV(t)}{dt} = \psi \cdot GV(t) \cdot \varphi(GV(t)) \tag{4}$$

where GV, ψ , and φ represent the growth rate, growth velocity, and correction factor for growth deviation, respectively. The member I_i is modeled by Equation (5).

$$\Delta GV_{i}(t+1) = rand^{2} \odot (N(1,D) \odot \Delta GV_{i}(t))$$
 (5)

where $GV_i(t)$ and $GV_i(t+1)$ represent the growth rates at discrete time steps t and t+1, respectively; *rand* is a random number in the range of [0,1]; N(1,D) represents a random vector of dimension D.

(3) Obtaining sunlight for growth. For ivy in nature, quickly finding a surface to attach to is crucial. The movement towards the light source is modeled by Equations (6)–(8). In the proposed algorithm, this behavior is simulated by the i — th individual I_i in the

Biomimetics **2025**, 10, 342 6 of 41

population, selecting its closest and most optimal neighbor I_{ii} (based on the value of the fitness function) as a reference for self-improvement, as shown in Figure 2.

$$I_{ii} = \begin{cases} I_{j-1}^{s}, I_{i} = I_{j}^{s} \\ I_{i}, I_{i} = I_{best} \end{cases}$$
 (6)

$$I_{i}^{\text{new1}} = I_{i} + |N(1, D)| \odot (I_{ii} - I_{i}) + N(1, D) \odot \Delta GV_{i}, i = 1, 2, \dots, N$$
(7)

$$\Delta Gv_{i} = \begin{cases} I_{i} \otimes (I_{max} - I_{min}), Iter = 1\\ rand^{2} \odot (N(1, D) \odot \Delta Gv_{i}), Iter > 1 \end{cases}$$
(8)

where |N(1,D)| is a vector, with each component being the absolute value of the corresponding component in the vector N(1,D).

(4) Growth and evolution of ivy. After the member I_i navigates the search space globally to reach its nearest and most significant neighbor I_{ii}, it enters a phase where I_i strives to directly follow the optimal member I_{best} in the population. This stage aligns with the pursuit of an improved optimal solution in the vicinity of I_{best}, as depicted in Equations (9) and (10).

$$I_{i}^{new} = I_{Best} \odot (rand(1, D) + N(1, D) \odot \Delta GV_{i})$$
 (9)

$$\Delta GV_{i}^{\text{new}} = I_{i}^{\text{new}} \otimes (I_{\text{max}} - I_{\text{min}}) \tag{10}$$

The flowchart of the ivy algorithm is shown in Figure 3.

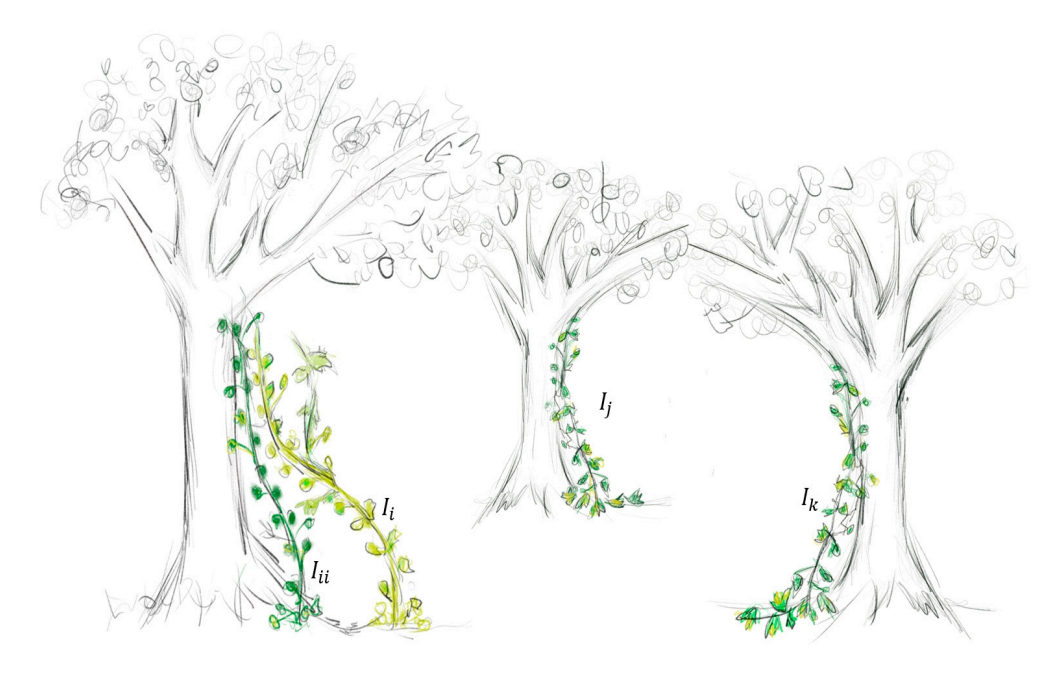


Figure 2. The i-th member of the population I_i chooses its closest, most vital neighbor I_{ii} .

Biomimetics **2025**, 10, 342 7 of 41

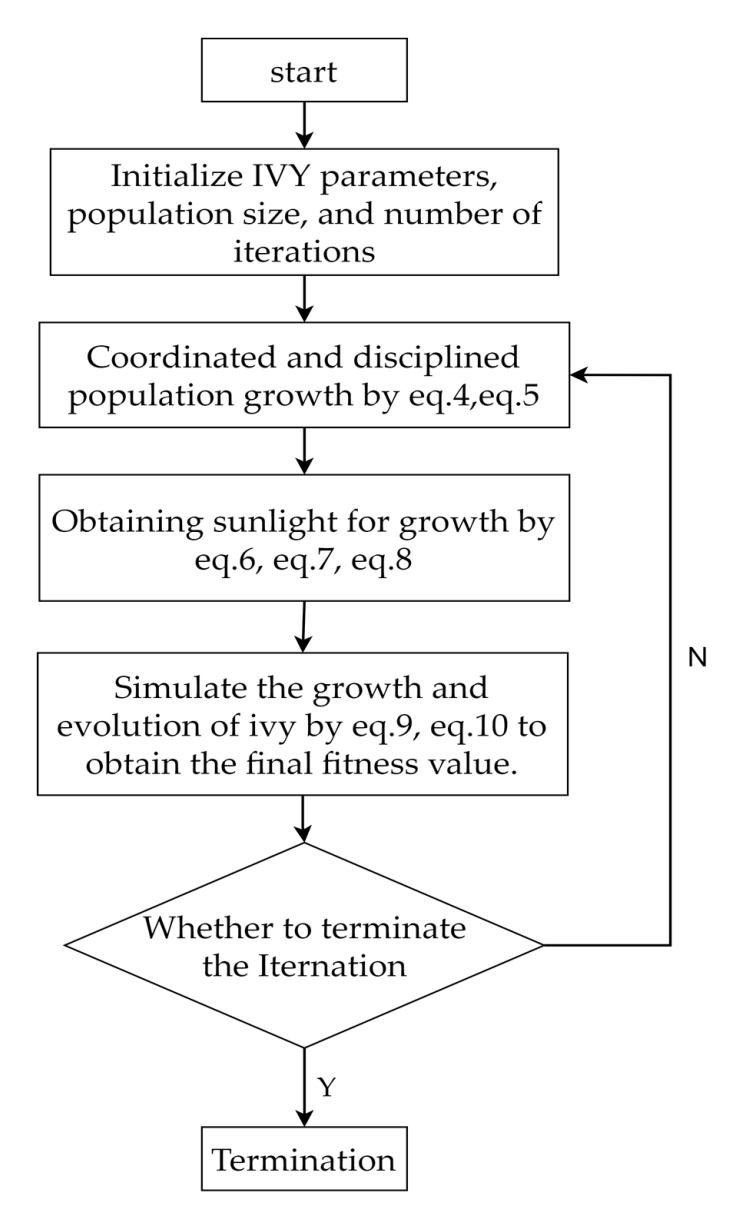


Figure 3. Flowchart of the ivy algorithm.

4. Proposed Optimization Formulation of IVYPSO

The IVYPSO hybrid algorithm integrates the global exploration capability of PSO with the local exploitation and adaptive perturbation mechanism inspired by the natural growth behavior of ivy plants. Specifically, the algorithm leverages the PSO's velocity-position update rule to guide individuals toward promising areas in the solution space. Meanwhile, an ivy-inspired *GV* introduces fine-grained random perturbations to enhance the local search capability around high-quality solutions. To balance exploration and exploitation, IVYPSO adaptively switches between global and local strategies based on a dynamic quality threshold. A greedy selection strategy is also employed to retain elite solutions in each iteration. This coordinated hybridization approach improves the convergence speed, avoids local optima, and enhances the solution's overall accuracy.

4.1. Initialization Phase

In this phase, the objective function fobj is defined to calculate the fitness. The lower and upper bounds of the search space, lb and ub, respectively, are set to restrict the solution range; N individuals are randomly generated, and the position and velocity

of each individual *i* are initialized, along with the ivy variables. The specific parameter initialization process is as follows.

The particles' initial positions in the search space are randomly generated, as described in Equation (11):

$$X_{i} = unifrnd(lb, ub, [1, dim]). \tag{11}$$

The velocity is initialized as a zero vector, as described in Equation (12):

$$V_i = zeros(1, dim). (12)$$

The ivy growth variable GV is then initialized, as described in Equation (13):

$$GV = \frac{X_{\rm i}}{ub - lb} \tag{13}$$

The ivy variable *GV* represents the relative growth behavior of an ivy plant within the bounded search space and is used to control the intensity of local random movement.

4.2. Guidance Mechanism: PSO-Guided Velocity Update

This step updates the velocity for each individual, as described by the velocity update formula in Equation (14):

$$V_i^{t+1} = w \cdot V_i^t + c_1 \cdot r_1 \cdot \left(P_{\text{best}} - X_i^t\right) + c_2 \cdot r_2 \cdot \left(G_{\text{best}} - X_i^t\right) \tag{14}$$

where w = 0.7, $c_1 = 1.5$, $c_2 = 1.5$, r_1 , and r_2 are randomly generated values within the interval [0, 1], adding randomness to the particles. This mechanism guides particles towards their personal best position P_{best} and the global best position G_{best} , promoting convergence toward high-quality areas.

This velocity update represents the guidance mechanism in a metaheuristic search (MHS), guiding particles toward personal and global best positions to balance exploration and exploitation. Recent state-of-the-art (SOTA) methods such as FDB and its variants improve the guidance by considering both the fitness and distance to avoid premature convergence.

4.3. Update Mechanism: Position Update with Ivy Perturbation

To achieve a dynamic balance between global and local searches, we introduce a dynamic control factor β_1 , which is a dynamic adjustment parameter that controls the ratio between global and local search. The expression is as described in Equation (15):

$$\beta_1 = 1 + \frac{rand}{2} \tag{15}$$

The random value rand is in the range of [0, 1], and the value of β_1 dynamically changes, which helps introduce randomness and balance the strengths of global and local searches. By adjusting β_1 , the algorithm primarily focuses on global searches in the early stages and gradually enhances the local search capability in the later stages, thereby improving the convergence accuracy.

In each iteration, for each individual I the update strategy is selected based on the relationship between its current fitness value $Cost(X_i)$ and the global best fitness value $Cost(G_{best})$. The condition judgment formula is as described in Equation (16):

$$Cost(X_i) < \beta_1 \cdot Cost(G_{best})$$
 (16)

where $Cost(X_i)$ represents the fitness value of the current individual and $Cost(G_{best})$ represents the fitness value of the current global best solution. If the condition is met, Equation (17) is used for local searches (exploited around a neighbor). Otherwise, Equation (18) is applied to global searches (perturbed toward the best). Equations (17) and (18) are as follows:

$$X'_{i} = x + \left| randn \right| \times \left(x_{neighbor} - x \right) + randn \times GV$$
 (17)

$$X_{i}^{'} = G_{best} \times (rand + randn \times GV)$$
(18)

Here, *GV* controls the perturbation magnitude; *randn* is a normally distributed random value that mimics the irregular yet directed growth of ivy tips toward better areas. The ivy growth variable is then updated using Equation (19).

$$GV = GV \times \left(rand^2 \times randn\right) \tag{19}$$

This adaptive update allows *GV* to decay or intensify based on the stochastic process, simulating flexible growth behaviors for refining solutions.

4.4. Survivor Selection Strategy

In metaheuristic search algorithms, survivor selection is a crucial component of the update mechanism that determines which individuals are retained in the population to balance the convergence speed and solution diversity. In IVYPSO, we employ a greedy selection strategy, described in Equation (20), to preserve improved solutions:

$$Cost(X_{i}^{'}) < Cost(X_{i}) \Longrightarrow X_{i}(t+1) = X_{i}^{'}$$
(20)

If the new position X_i yields a better fitness than the current position X_i , it replaces the current solution; otherwise, the original solution is retained. Additionally, the individual best $P_{\text{best},i}$ and global best G_{best} are updated synchronously upon improvement.

Furthermore, inspired by recent advances in metaheuristics, the NSM has been proposed as an effective survivor selection technique. NSM dynamically combines fitness and historical success information to select survivors, enhancing the stability and diversity in the population. Although IVYPSO does not explicitly implement NSM, its greedy selection strategy combined with ivy-inspired perturbations shares conceptual similarities with NSM's goal of balancing exploitation and exploration, ensuring robustness against premature convergence. Future work may explore integrating NSM directly into IVYPSO to further improve the update mechanism performance.

4.5. Summary

Through PSO-guided global movement and ivy-inspired local perturbations, IVYPSO forms a complementary hybrid search system. The use of ivy growth variables enhances the adaptability and solution refinement, particularly in rugged or complex landscapes. The implementation process of IVYPSO is illustrated in Figure 4 and Algorithm 1.

Algorithm 1. IVYPSO

```
Input: N, Max_iteration, lb, ub, dim, fobj
Output: Destination_fitness, Destination_position, Convergence_curve
Initialize parameters:
         Set PSO parameters: inertia weight (w), cognitive factor (c1), social factor (c2)
         Initialize population size (N), maximum iterations (Max_iteration), search
space (lb, ub)
         Define and initialize the vine growth variable (GV)
Initialize population:
         For each particle i in population:
                  Randomly initialize position Position_i within [lb, ub]
                  Initialize velocity Velocity_i as a zero vector
                  Evaluate fitness Cost_i = fobj(Position_i)
                  Initialize vine growth variable GV_i = Position_i/(ub - lb)
                  Set personal best PBest_i = Position_i and PBest_Cost_i = Cost_i
         Set global best GBest as the particle with the lowest fitness value
Iteration loop (t = 1 to Max_iteration):
         For each particle i in population:
                  Update velocity and position:
                           Generate random vectors r1 and r2
                           Velocity_i = w * Velocity_i
                                     + c1 * r1 * (PBest_i - Position_i)
                                     + c2 * r2 * (GBest - Position_i)
                  Calculate dynamic control factor \beta:
                       \beta = 1 + (random/2)
                  Perform local or global search based on fitness comparison:
                       If Cost_i < \beta * GBest_Cost:
                           New_Position = Position_i
                                              + |N(0,1)| * (Position_neighbor -
Position i)
                                              + N(0,1) * GV_i
                       Else:
                           New_Position = GBest * (random + N(0,1) * GV_i)
                  Boundary handling:
                       Ensure New_Position is within [lb, ub]
                  Update vine growth variable:
                       GV_i = GV_i * (random^2 * N(0,1))
                  Evaluate and update solutions:
                       New_Cost = fobj(New_Position)
                       If New_Cost < Cost_i:
                           Position_i = New_Position
                           Cost_i = New_Cost
                           If New_Cost < PBest_Cost_i:</pre>
                                     PBest_i = New_Position
                                     PBest_Cost_i = New_Cost
                                     If New_Cost < GBest_Cost:
                                              GBest = New Position
                                              GBest\_Cost = New\_Cost
         Record the best fitness at the current iteration:
                  Convergence_curve(t) = GBest_Cost
Return:
         Destination_fitness = GBest_Cost
         Destination_position = GBest
         Convergence_curve
```

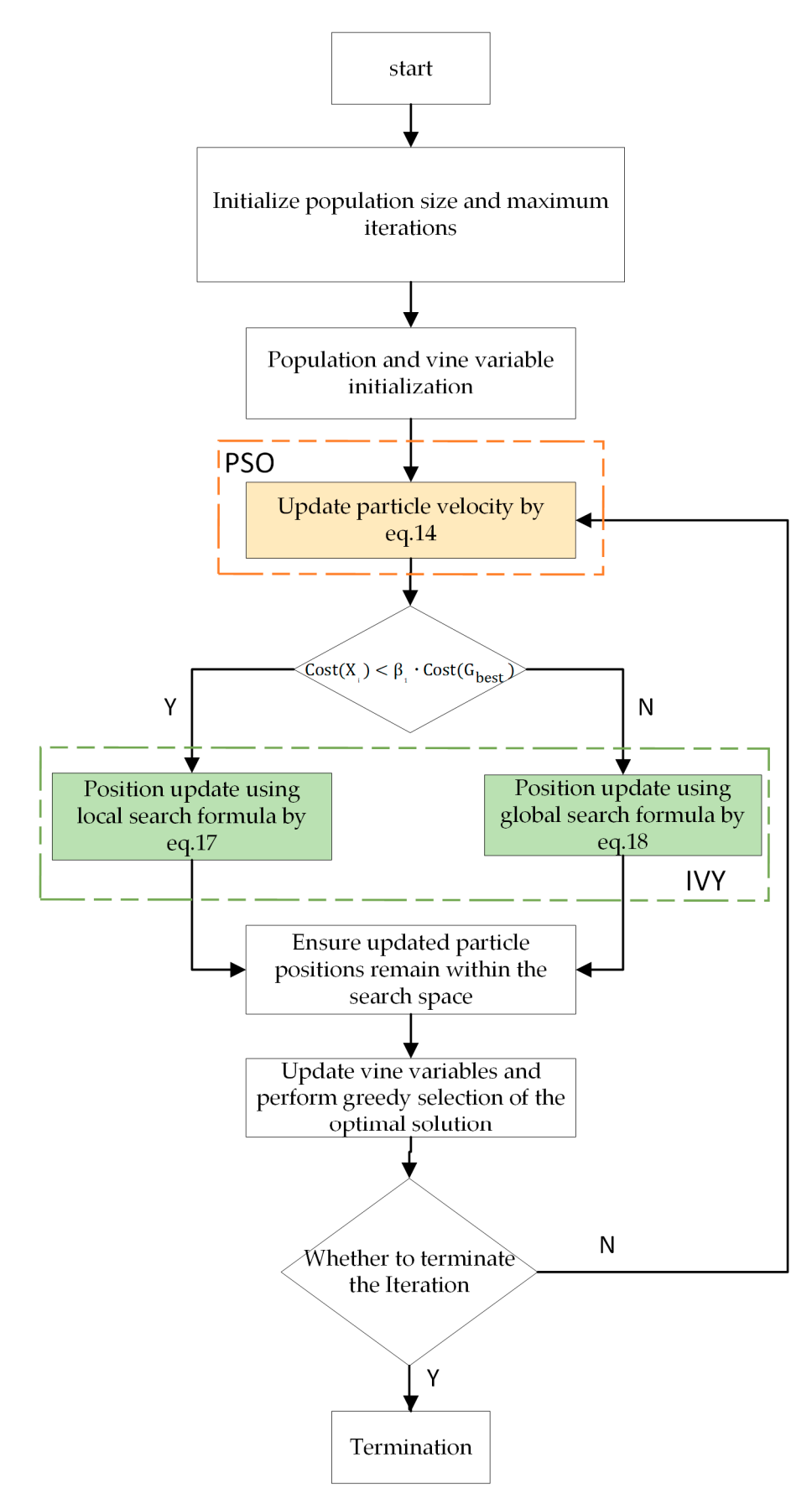


Figure 4. Flowchart of IVYPSO algorithm.

5. Results and Analytical Evaluation of the Experiment

To verify the proposed algorithm's reliability and performance, 26 standard benchmark functions were utilized. Moreover, we applied the algorithm to three real-world engineering optimization problems to evaluate its practical performance. The subsequent sections offer comprehensive details on the benchmark functions, parameter configurations, and performance metrics. The algorithm's effectiveness was assessed through a comparative analysis with ten widely recognized metaheuristic algorithms.

Setup for experiments: The proposed IVYPSO algorithm and other metaheuristic methods were implemented in MATLAB 2023a. All tests were conducted on a Windows 10 platform with an Intel(R) Core (TM) i9-14900KF processor (3.10 GHz) and 32 GB of RAM.

5.1. Global Optimization with 26 Benchmark Mathematical Test Functions

To assess the performance of the proposed IVYPSO algorithm in solving complex optimization problems, this study employed 26 widely recognized benchmark functions [34–36]. These functions were selected to ensure a comprehensive evaluation covering various optimization scenarios, and they are grouped here into two main categories: unimodal and multimodal functions. Each function was tested in a 30-dimensional space.

Unimodal functions: The initial set of 15 benchmark functions (F1–F15) is unimodal, characterized by the presence of a single global optimum, making it suitable for evaluating the convergence speed and local exploitation capability of optimization algorithms. These functions provide a smooth search landscape without local optima, allowing the assessment of an algorithm's ability to quickly converge to the global minimum.

For instance, the Quartic function introduces a noise component that simulates real-world measurement errors, making it relevant for applications such as experimental data fitting. The Sum Power function, with its amplified penalization of higher-order dimensions, reflects challenges seen in structural reliability or robust design tasks in engineering optimization.

Multimodal functions: The latter set of functions (F16–F26) is multimodal, containing numerous local optima and being employed to test an algorithm's ability to maintain diversity and avoid premature convergence. These functions simulate complex landscapes typically encountered in real-world scenarios such as material design, resource allocation, or non-linear process optimization.

For example, the Alpine function represents rugged fitness landscapes with a repetitive pattern, akin to multi-peak phenomena in signal processing or energy system optimization. The Weierstrass function, characterized by its fractal-like structure, is often used to test algorithms under highly irregular and non-differentiable conditions, making it applicable to domains such as financial modeling or dynamic system tuning.

By adopting this comprehensive set of 26 benchmark functions, this study evaluated IVYPSO across a wide range of conditions, from simple landscapes to highly complex multimodal terrains. This thorough testing ensures that the algorithm's effectiveness, robustness, and generalization ability were rigorously validated. The full mathematical formulations and parameter settings of the benchmark functions are detailed in Table 1.

Table 1. Details of the 26 test functions.

s/n	Function Name	Formula	Category	Range	f_{min}^{*}
F1	Sphere	$f_1(x) = \sum_{i=1}^{\dim x} x_i^2$	Unimodal	[-100, 100]	0
F2	Schwefel 2.22	$f_1(x) = \sum\limits_{i=1}^{\dim} x_i^2 \ f_2(x) = \sum\limits_{i=1}^{\dim} \left x_i \right + \prod\limits_{i=1}^{\dim} \left x_i \right $	Unimodal	[-10, 10]	0
F3	Schwefel 1.2	$f_3(x) = \sum_{i=1}^{i=1} \left(\int_{i}^{i} x_i \right)^2$	Unimodal	[-100, 100]	0
F4	Schwefel 2.21	$f_3(x) = \sum_{i=1}^{\dim} \left(\sum_{j=1}^i x_j\right)^2$ $f_4(x) = \max_i \{ x_i \}, 1 \le i \le \dim$	Unimodal	[-100, 100]	0
F5	Step	$f_5(x) = \sum_{i=1}^{dim} (x_i + 0.5)^2$	Unimodal	[-100, 100]	0
F6	Quartic	$f_6(x) = \sum_{i=1}^{i=1} i x_i^4 + \text{rand}$	Unimodal	[-1.28, 1.28]	0
F7	Exponential	$f_{7}(x)=\sum\limits_{i=1}^{i=1} \stackrel{\mathrm{dim}}{\mathrm{dim}} (e^{x_{i}}-x_{i})$	Unimodal	[-10, 10]	0
F8	Sum power	$f_8(x) = \sum_{i=1}^{i=1} x_i^2$	Unimodal	[-1, 1]	0
F9	Sum square	$f_9(x) = \sum_{i=1}^{i=1} \frac{\sin^2 x}{ix_i^2}$	Unimodal	[-10, 10]	0
F10	Rosenbrock	$f_{10}(x) = \sum_{i=1}^{\dim -1} \left(100(x_{i+1} - x_i^2)^2 + (x_i - 1)^2 \right)$	Unimodal	[-5, 10]	0
F11	Zakharov	$f_{11}(x) = \underbrace{\lim_{i=1}^{i=1} x_i^2}_{i} + \left(\frac{\lim_{i \to 0} 0.5ix_i}{\sum_{i=1}^{i} 0.5ix_i}\right)^2 + \left(\frac{\lim_{i \to 0} 0.5ix_i}{\sum_{i=1}^{i} 0.5ix_i}\right)^4$	Unimodal	[-5, 10]	0
F12	Trid	$f_{12}(x) = \int_{-1}^{\text{dim}} \int_{-1}^{(i=1)} \int_{-1}^{(i=1)} \int_{-1}^{(i=1)} f_{12}(x) dx$	Unimodal	[-5, 10]	0
F13	Elliptic	$f_{13}(x) = \sum_{i=1}^{i=1} (10^6)^{i/(\dim -1)} x_i^2$	Unimodal	[-100, 100]	0
F14	Cigar	$f_{14}(x) = x_1^2 + 10^6 \sum_{i=1}^{\text{dim}} x_i^2$	Unimodal	[-100, 100]	0
F15	Rastrigin	$f_{15}(x) = \sum_{i=1}^{\dim} (x_i^2 - 10\cos(2\pi x_i) + 10)$	Fixed	[-5.12, 5.12]	0
F16	NCRastrigin	$f_{16}(x) = \sum_{i=1}^{\dim} (x_i^2 - 10\cos(2\pi x_i) + 10), y_i = \begin{cases} x_i, & \text{if } x_i \le 0.5\\ x_i - 1, & \text{otherwise} \end{cases}$	Multimodal	[-5.12, 5.12]	0
F17	Ackley	$f_{17}(x) = 20e^{-0.2\sqrt{\frac{1}{\dim\sum_{i=1}^{\dim x_i^2}} x_i^2}} + e^{-1}\sum_{i=1}^{\dim \cos(2\pi x_i) + 20 + e}$	Multimodal	[-50, 50]	0
F18	Griewank	$f_{18}(x) = 1 + \frac{1}{4000} \sum_{i=1}^{\dim} x_i^2 - \prod_{i=1}^{i=1} \cos\left(\frac{x_i}{\sqrt{i}}\right)$	Multimodal	[-600, 600]	0
F19	Alpine	$f_{19}(x) = \sum_{i=1}^{\dim} \begin{vmatrix} x_i \sin(x_i) + 0.1x_i \end{vmatrix}$	Fixed	[-10, 10]	0
F20	Penalized 1	$f_{20}(x) = \frac{f_{20}(x)}{\dim \left\{ 10\sin^2(\pi y_1) + \sum_{i=1}^{\dim - 1} \left(y_i - 1 \right)^2 \left[1 + 10\sin^2(\pi y_{i+1}) \right] + \left(y_{\dim} - 1 \right)^2 \right\} + \sum_{i=1}^{\dim } u(x_i, 10, 100, 4), y_i = 1 + \frac{x_i + 1}{4}, u(x_i, a, k, m) = \begin{cases} k(x_i - a)^m, & x_i > a \\ 0, & -a \le x_i \le a \\ k(-x_i - a)^m, & x_i < -a \end{cases}$	Multimodal	[-100, 100]	0
F21	Penalized 2	$f_{21}(x) = 0.1 \left\{ \sin^2(3\pi x_1) + \sum_{i=1}^{\dim - 1} \left(x_i - 1 \right)^2 \left[1 + \sin^2(3\pi x_{i+1}) \right] + \left(x_{\dim} - 1 \right)^2 \left[1 + \sin^2(2\pi x_{\dim}) \right] \right\} + \sum_{i=1}^{\dim} u(x_i, 5, 100, 4)$	Multimodal	[-100, 100]	0
F22	Schwefel	$f_{22}(x) = \sum_{i=1}^{\dim} x_i \sin\left(\sqrt{ x_i }\right)$	Fixed	[-100, 100]	0
F23	Lévy	$f_{23}(x) = \sin^2(3\pi x_1) + \sum_{i=1}^{\dim} \left(x_i - 1 \right)^2 \left[1 + \sin^2(3\pi x_{i+1}) \right] + \left(x_{\dim} - 1 \right)^2 \left[1 + \sin^2(2\pi x_{\dim}) \right]$	Multimodal	[-10, 10]	0
F24	Weierstrass	$f_{24}(x) = \sum_{i=1}^{\dim} \left(\sum_{k=0}^{k_{max}} a^k \cos(2\pi b^k (x_i + 0.5)) \right) - \dim \left(\sum_{k=0}^{k_{max}} a^k \cos(\pi b^k) \right), a = 0.5, b = 3, k_{max} = 20$	Multimodal	[-0.5, 0.5]	0
F25	Solomon	$f_{25}(x) = 1 - \cos\left(2\pi\sqrt{\sum_{i=1}^{\dim x} x_i^2}\right) + 0.1\sqrt{\sum_{i=1}^{\dim x} x_i^2}$	Fixed	[-100,100]	0
F26	Bohachevsky	$f_{26}(x) = \sum_{i=1}^{\dim} (x_i^2 + 2x_i^2 - 0.3\cos(3\pi x_i))$	Fixed	[-10,10]	0

Biomimetics 2025, 10, 342 14 of 41

5.1.1. Performance Indicators

To objectively assess the effectiveness of the IVYPSO algorithm, this study used the following standard evaluation metrics to comprehensively assess its performance across different benchmark tests [37–40].

Average value (Avg): The average fitness value obtained from M independent runs of the algorithm, calculated as shown in Equation (21).

$$Avg = \frac{\sum_{i=1}^{M} (f_i)}{M}$$
 (21)

Standard deviation (Std): The variability in the objective function values obtained from M independent runs of the algorithm. The standard deviation is calculated using Equation (22).

$$Std = \sqrt{\frac{1}{M-1} \sum_{i=1}^{M} (f_i - Avg)^2}$$
 (22)

Best: The minimum fitness obtained from M independent runs of the algorithm, as shown in Equation (23).

$$Best = \min_{1 \le i \le M} f_i \tag{23}$$

where f_i denotes the optimal fitness value attained during run i.

5.1.2. Parameter Settings and Performance Comparison Against Other Algorithms

Table 2 summarizes the parameter settings for the IVYPSO algorithm and its compari-

son algorithms. The proper adjustment of the parameters for each algorithm is crucial to
ensure optimal performance. To maintain the fairness of the comparison, the initial settings
and common parameters for all algorithms are set based on the standard values from the
existing literature, while the remaining parameters are optimized through experimental
procedures. The comparison algorithms selected in this study include classic metaheuristic
methods such as PSO, IVY, BOA [41], and WOA [42], as well as several recently proposed
improved algorithms, including GOOSE and HPSOBOA, and several advanced variant
algorithms such as FDC-AGDE, dFDB-LSHADE, NSM-BO, dFDB-SFS, and FDB-AGSK.
These algorithms have demonstrated strong performance in the IEEE CEC competition and
in solving real-world engineering optimization problems. In this study, the evaluation of
the objective function is terminated upon reaching the maximum number of iterations.

Algorithm	Parameter	Algorithm	Parameter
ALL	Max iteration = 500, Agents = 30, Runs = 30	HPSOBOA	$w = 0.7, a = (0.1, 0.3), V = (-1, 1), C_1 = C_2 = 0.5, c_0 = 0.01, p = 0.6$
IVYPSO	$C_1 = C_2 = 1.5, w = 0.7, beta_1 = [1, 1.5), GV = [0, 1]$	dFDB_LSHADE	$p_best_rate = 0.11$, $arc_rate = 1.4$ $memory_size = 5$, $memory_pos = 1$
PSO	$C_1 = C_2 = 2, V = (-6, 6), w = (0.2, 0.9)$	FDC_AGDE	$NW = [0.5 \ 0.5] \cdot Cr \ All = zeros(1.2)$
IVY BOA	$beta_1 = [1, 1.5), \text{ GV} = [0, 1]$ $a = 0.1, p = 0.6, c_0 = 0.01$	NSM_BO	$p_{xgm_{initial}} = 0.03, scab = 1.25, scsb = 1.3$
WOA	a = linear decrease from 2 to 0, C = [0, 2], a2 = linear decrease from -1 to -2	dFDB_SFS	$rcpp = 0.0035, tsgs_factor_max = 0.05$ $d = X(A,:) - X(\overline{B},:)$
GOOSE	S_W_min = 5, S_W_max = 25, coe_min = 0.17	FDB_AGSK	l = rand()*2 - 1, b = 1

Table 2. Parameter settings of IVYPSO and other algorithms.

5.1.3. Analysis of Numerical Results

The proposed algorithm's performance was evaluated and compared with several mature and latest algorithms.

Table 3 presents a detailed comparison of the average fitness values and standard deviations achieved by the IVYPSO algorithm and other algorithms across the test functions.

Notably, IVYPSO attained the best average fitness on 21 out of the 26 test functions (F1–F4, F6, F8–F20, F24–F26), outperforming the other 11 algorithms. Particularly impressive was its performance on 17 functions (F1–F4, F8, F9, F11, F13–F17, F19, F20, F24–F26), where it achieved the best average fitness with a standard deviation of zero, demonstrating excellent stability and efficiency. On functions F5, F21, and F23, the IVYPSO algorithm ranked 6th, 5th, and 4th, respectively. However, its performance on F7 and F22 was relatively poor, ranking 11th and 12th, respectively.

Table 4 compares the best fitness values obtained by the IVYPSO algorithm and the other 11 algorithms across the test functions. Among the 26 functions, IVYPSO achieved superior results on 20 functions (F1–F4, F8, F9, F11–F20, F24–F26), outperforming the other 11 algorithms. For functions F6, F21, and F23, IVYPSO ranked 2nd, 4th, and 2nd, respectively, in terms of the best fitness value. Nevertheless, its performance was inferior on functions F5, F7, and F22, where it ranked 8th, 11th, and 10th, respectively.

In summary, the IVYPSO algorithm can be considered a superior optimization algorithm.

5.1.4. Analysis of Convergence Behavior

Figure 5 compares the convergence behavior of the IVYPSO algorithm with that of other algorithms over 500 iterations. The vertical axis represents the best fitness value obtained at each iteration, while the horizontal axis indicates the iteration count. On 16 out of the 26 test functions (specifically F1–F4, F6, F8–F15, F18, F20, and F25), IVYPSO demonstrated consistently faster and more efficient convergence, outperforming the other algorithms. Although IVYPSO exhibits strong global optimization capability, a few other algorithms outperformed it in certain specific cases.

5.1.5. Analysis of Exploitation Capabilities

Ideal for evaluating the algorithm's development capabilities, the single-modal benchmark functions (F1–F14) contain only one minimum. For functions F1–F4, F8, F9, F11, F13, and F14, Figure 3 demonstrates that IVYPSO reaches the theoretical best solution in around 50 iterations. Reflecting IVYPSO's high precision and stability, Table 3 reveals that the average fitness and standard deviation for these functions are typically 0. These findings clearly indicate that IVYPSO outperforms most of the comparison algorithms on the benchmark functions. For the multi-modal functions F15–F17, F19, F20, and F24–F26, IVYPSO also attains the theoretical best fitness in around 50 iterations. Table 4 demonstrates that the majority of the algorithms are capable of locating the theoretical optimal solution. Moreover, Table 3 underscores that IVYPSO demonstrates better average fitness and standard deviation than most competing algorithms, highlighting its robust and stable exploration capabilities.

5.1.6. Wilcoxon Signed-Rank Analysis Results and Friedman Ranking Scores

To ensure statistically robust conclusions, the widely accepted Wilcoxon non-parametric [43–46] test was used to assess the effectiveness of IVYPSO compared to 11 other algorithms. Table 5 presents the results of the Wilcoxon signed-rank test applied to 26 standard test functions at a significance level of $\alpha = 0.05$, using the mean objective value of each function as the test sample. The p-value, which reflects the significance level, is considered significant when below 0.05. The data in Table 5 show that IVYPSO yields p-values below 0.05 in all cases. Therefore, this analysis statistically validates the superiority of IVYPSO over the other 11 algorithms.

Table 3. A comparison of IVYPSO's average fitness values and standard deviation with 10 other algorithms for various test functions.

Func	Metrics	IVYPSO	PSO	IVY	BOA	WOA	GOOSE	HPSOBOA	dFDB_LSHADE	FDC_AGDE	NSM_BO	dFDB_SFS	FDB_AGSK
F1	Avg	0	2.5159	5.6148×10^{-160}	7.5380×10^{-11}	4.4643×10^{-74}	28.045	1.6444×10^{-291}	4954.6436	6.1553×10^{-3}	0.5044	27.5647	6.0516×10^{-96}
	Std	0	1.1071	8.5891×10^{-160}	7.0143×10^{-12}	2.2966×10^{-73}	103.4571	0	1398.5169	3.6651×10^{-3}	1.982	10.3053	3.3035×10^{-95}
	Rank	1	9	3	6	5	11	2	12	7	8	10	4
F2	Avg	0	4.5489	0	2.3029×10^{-8}	2.5328×10^{-50}	1359.2299	1.0782×10^{-145}	43.1042	1.4138×10^{-2}	4.2033×10^{-3}	4.5363	3.9126×10^{-60}
	Std	0	1.1878	0	6.7460×10^{-9}	1.3725×10^{-49}	6860.7534	7.0216×10^{-146}	9.4746	3.4474×10^{-3}	8.0123×10^{-3}	1.1547	2.1335×10^{-59}
	Rank	1	10	1	6	5	12	3	11	8	7	9	4
F3	Avg	0	82.4665	5.6472×10^{-85}	5.2628×10^{-11}	422.432	2.43	3.3155×10^{-292}	188.7533	8.4739	3.6188	174.9405	419.0353
	Std	0	24.2503	4.3479×10^{-86}	6.0949×10^{-12}	156.2203	0.8986	0	78.0896	13.0659	3.9852	48.3456	128.6289
	Rank	1	8	3	4	12	5	2	10	7	6	9	11
F4	Avg	0	1.9179	0	2.6176×10^{-8}	3.8852	0.2502	5.4053×10^{-147}	4.4093	1.2657	2.2818	1.1509	5.7175
	Std	0	0.32	0	2.4363×10^{-9}	2.8659	0.2304	3.3527×10^{-148}	0.744	0.1467	0.4925	0.2463	3.5226
	Rank	1	8	1	4	10	5	3	11	7 _	9	6	12
F5	Avg	0.241	2.2492	0.4888	5.3766	9.8934×10^{-2}	0.0114	0.0327	53.3583	6.2779×10^{-5}	3.2036×10^{-3}	0.2562	0.5742
	Std	0.1957	1.1515	0.4037	0.4651	7.3668×10^{-2}	3.7831×10^{-3}	2.3514×10^{-2}	16.69	3.1763×10^{-5}	7.9615×10^{-3}	8.6912×10^{-2}	0.5068
	Rank	6	10	8	11	5	3	4	12	1	2	7	9
F6	Avg	6.7137×10^{-5}	14.4701	6.7440×10^{-5}	1.9729×10^{-3}	2.5420×10^{-3}	0.1336	1.1522×10^{-4}	1.9443	6.3089×10^{-2}	0.0984	7.7676×10^{-2}	1.3547×10^{-3}
	Std	5.9831×10^{-5}	10.0623	6.4272×10^{-5}	8.4663×10^{-4}	3.0980×10^{-3}	4.2711×10^{-2}	8.8115×10^{-5}	0.8096	1.4809×10^{-2}	3.9632×10^{-2}	2.4921×10^{-2}	2.5808×10^{-3}
	Rank	1	12	2	5	6	10	3	11	7	9	8	4
F7	Avg	4.8103×10^{-15}	0	8.7899×10^{-31}	6.3334×10^{-11}	7.1751×10^{-66}	1.2216×10^{-65}	1.7703×10^{-62}	1.6598×10^{-48}	2.5562×10^{-54}	7.1751×10^{-66}	2.0229×10^{-65}	7.1751×10^{-66}
	Std	1.7831×10^{-14}	0	4.0250×10^{-30}	2.0811×10^{-10}	3.2167×10^{-81}	1.6721×10^{-65}	8.7838×10^{-78}	9.0229×10^{-48}	1.3999×10^{-53}	3.2167×10^{-81}	1.2398×10^{-65}	3.2167×10^{-81}
	Rank	11	1	10	12	2	5	7	9	8	3	6	4
F8	Avg	0	0.183	0	9.7665×10^{-14}	3.5039×10^{-104}	1.7042×10^{-5}	1.2449×10^{-295}	7.6028×10^{-4}	9.4531×10^{-20}	2.5527×10^{-20}	1.4060×10^{-10}	4.4055×10^{-153}
	Std	0	0.1684	0	6.2767×10^{-14}	1.9152×10^{-103}	1.1127×10^{-5}	0	1.5541×10^{-3}	3.4998×10^{-19}	8.9169×10^{-20}	3.8320×10^{-10}	2.3589×10^{-152}
-	Rank	1	12	1	8	5 72	10	3	11	7	6	9	4
F9	Avg	0	26.7969	4.3686×10^{-95}	6.8638×10^{-11}	2.6339×10^{-73}	0.8848	2.6080×10^{-291}	658.4361	6.9232×10^{-4}	0.123	2.9677	1.3465×10^{-94}
	Std	0	14.5494	0	5.7608×10^{-12}	1.4319×10^{-72}	0.7549	0	209.486	4.2068×10^{-4}	0.4863	0.9921	5.1291×10^{-94}
F10	Rank	1 26.9025	11 914.4537	3 27.6343	6 28.9104	5 27.9035	9 86.349	2 28.7569	12 45,111.5779	7 60.6339	8 87.2424	10 162.7128	4 28.7208
F10	Avg Std	0.8425	438.8139	0.2558	2.3631×10^{-2}	0.4628	68.1133	4.3639×10^{-2}	29,206.2521	43.6974	53.4909	63.2633	9.4422×10^{-2}
	Rank	1	430.0139	2	2.3631 × 10 -	3	8	4.3639 × 10 =	12	7	9	10	9.4422 × 10 - 4
F11	Avg	0	111.8508	0	6.6299×10^{-11}	7.0248×10^{-75}	0.1491	1.5401×10^{-291}	679.9458	6.8789×10^{-4}	9.7422×10^{-3}	1.7317	2.7436×10^{-92}
111	Std	0	52.0599	0	6.5461×10^{-12}	2.5674×10^{-74}	3.6406×10^{-2}	0	337.3768	3.7684×10^{-4}	1.8844×10^{-2}	0.5826	1.5027×10^{-91}
	Rank	1	11	1	6.5461 × 10	2.3674 × 10 5	3.0400 × 10	3	12	7	1.00 11 × 10 8	10	1.5027 × 10
F12	Avg	0.6667	209.9059	0.6667	0.9707	0.667	2.1609	0.9959	1233.9148	0.8234	2.9415	3.9169	0.7818
	Std	9.4147×10^{-8}	128.9306	4.7975×10^{-8}	9.8902×10^{-3}	2.0518×10^{-4}	1.3914	8.0022×10^{-4}	870.8841	0.2879	1.8042	1.7217	0.1635
	Rank	1	11	2	6	3	8	7	12	5	9	10	4
F13	Avg	0	1.7597×10^{-23}	0	1.2000×10^{-21}	0	3.3757×10^{-4}	5.2516×10^{-2}	8.6767	8.4768×10^{-37}	0	1.8101×10^{-32}	0
	Std	0	9.2757×10^{-23}	0	3.9643×10^{-21}	0	5.2807×10^{-4}	0.103	17.2354	3.6192×10^{-36}	0	4.8001×10^{-32}	0
	Rank	1	8	1	9	1	10	11	12	6	1	7	1
F14	Avg	0	1.2617×10^{-17}	0	6.5631×10^{-15}	2.0239×10^{-103}	1997.0369	0.0359	8.1314	2.6242×10^{-25}	0	2.3759×10^{-19}	9.7815×10^{-151}
	Std	0	4.3869×10^{-17}	0	3.5821×10^{-14}	9.0242×10^{-103}	2107.4933	0.1044	23.3506	1.4323×10^{-24}	0	5.3197×10^{-19}	5.3566×10^{-150}
	Rank	1	8	1	9	5	12	10	11	6	1	7	4
F15	Avg	0	1.0826×10^{-23}	5.3697×10^{-260}	1.3855×10^{-18}	1.1287×10^{-128}	6.8549×10^{-3}	3.1054×10^{-3}	0.0557	1.6634×10^{-36}	0	1.8751×10^{-30}	1.6475×10^{-192}
	Std	0	4.3883×10^{-23}	6.3684×10^{-259}	4.4188×10^{-18}	6.1811×10^{-128}	1.1247×10^{-2}	6.5997×10^{-3}	0.1444	9.0070×10^{-36}	0	5.4607×10^{-30}	0
	Rank	1	8	3	9	5	11	10	12	6	ĭ	7	4
F16	Avg	0	169.139	0	26.6377	0	150.3139	0.3609	239.6035	46.6483	10.3208	214.2906	1.8948×10^{-15}
	Std	0	31.3264	0	69.0482	0	28.026	0.8057	18.0974	7.1298	3.6033	14.3203	1.0378×10^{-14}
	Rank	1	10	1	7	ĺ	9	5	12	8	6	11	4
F17	Avg Std	0	151.8179	Ō	109.6198	4.9084	194.1359	0.2559	216.455	30.7778	8.7194	197.9083	0
		0	28.435	0	79.6068	26.8846	33.0475	0.4747	23.1197	3.1702	3.0756	19.4055	0
	Rank	1	9	1	8	5	10	4	12	7	6	11	1

 Table 3. Cont.

Func	Metrics	IVYPSO	PSO	IVY	BOA	WOA	GOOSE	HPSOBOA	dFDB_LSHADE	FDC_AGDE	NSM_BO	dFDB_SFS	FDB_AGSK
F18	Avg	4.4409×10^{-16}	2.5742	4.4409×10^{-16}	2.7789×10^{-8}	3.1678×10^{-15}	8.1913	4.4409×10^{-16}	9.3502	1.2613×10^{-2}	0.8511	2.3255	3.6415×10^{-15}
	Std	0	0.4745	0	2.7043×10^{-9}	2.5861×10^{-15}	7.6507	0	0.946	3.3014×10^{-3}	0.6142	0.4014	2.1580×10^{-15}
	Rank	1	10	1	6	4	11	1	12	7	8	9	5
F19	Avg	0	0.1297	8.3647×10^{-31}	1.0441×10^{-11}	9.3855×10^{-3}	240.6283	0	51.1922	5.7896×10^{-2}	0.1998	1.2171	5.3087×10^{-2}
	Std	0	5.8069×10^{-02}	9.1238×10^{-30}	8.8748×10^{-12}	3.6288×10^{-2}	219.7319	0	16.6066	5.7987×10^{-2}	0.2448	9.1563×10^{-2}	0.2087
	Rank	1	8	3	4	5	12	1	11	7	9	10	6
F20	Avg	0	5.5514	0	2.9520×10^{-9}	1.0727×10^{-44}	6.33	4.9382×10^{-147}	25.9518	3.0941×10^{-2}	1.1060×10^{-3}	10.4077	2.4419×10^{-62}
	Std	0	2.3383	0	8.8910×10^{-9}	5.8751×10^{-44}	2.6195	6.0974×10^{-147}	4.7219	1.0909×10^{-2}	1.6310×10^{-3}	2.5345	6.5463×10^{-62}
	Rank	1	9	1	6	5	10	3	12	8	7	11	4
F21	Avg	2.5547×10^{-2}	5.2594×10^{-2}	2.9661×10^{-2}	0.5326	1.9728×10^{-2}	3.8312	2.2408×10^{-3}	3.2529	4.4463×10^{-6}	2.0755×10^{-2}	0.0312	3.5037×10^{-2}
	Std	9.7752×10^{-3}	4.9296×10^{-2}	1.4688×10^{-2}	0.1176	5.4402×10^{-2}	1.3479	1.6259×10^{-3}	1.2921	4.5629×10^{-6}	4.2171×10^{-2}	2.6494×10^{-2}	0.03
	Rank	5	9	4	10	3	12	2	11	1	4	6	7
F22	Avg	2.9038	0.5688	2.9005	2.7472	0.1729	9.1851×10^{-3}	1.0042	2.7355	4.4222×10^{-6}	5.5565×10^{-3}	4.5368×10^{-2}	0.134
	Std	0.1621	0.247	0.19955	0.3013	0.1276	6.9460×10^{-3}	0.8045	0.8778	5.7875×10^{-6}	1.0655×10^{-2}	1.8046×10^{-2}	0.0886
	Rank	12	7	9	10	6	3	8	9	1	2	4	5
F23	Avg	0.5537	6.2603	1.3854	12.1723	0.3206	0.8029	0.7788	5.8924	3.9947×10^{-2}	6.3801×10^{-2}	1.6454	0.5537
	Std	1.1402	3.5956	0.8307	2.4477	0.2835	0.6338	0.8349	1.7669	0.012	8.4765×10^{-2}	0.6333	1.1402
	Rank	4	11	5	12	3	6	5	10	1	2	9	4
F24	Avg	0	3.7947	8.1486×10^{-8}	1.0973	0	9.6985	0	38.4245	0	1.4924×10^{-5}	0	0
	Std	0	3.1278	8.6874×10^{-8}	2.0728	0	6.5506	0	2.5571	0	5.6480×10^{-5}	0	0
	Rank	1	10	7	9	3	11	4	12	5	8	6	7
F25	Avg	0	1.6918	0	0.714	0.1592	1.844	0.0233	20.7438	0.732	4.9581	1.0114	0.136
	Stď	0	0.4571	0	0.2408	0.1373	0.4942	4.2871×10^{-2}	6.4717	0.2354	1.5861	0.2408	0.1394
	Rank	1	9	1	6	5	10	3	12	7	11	8	4
F26	Avg	0	22.3883	0	7.8537×10^{-11}	0	4.9249	0	58.728	1.6200×10^{-2}	0.4135	4.5409	0
	Std	0	6.0981	0	8.3251×10^{-12}	0	2.077	0	12.0427	8.5765×10^{-2}	1.0675	1.4705	0
	Rank	1	11	1	6	1	10	1	12	7	8	9	1
	Paired rar		24/0/2	11/12/3	25/0/1	18/3/5	23/0/3	19/3/4	24/0/2	21/0/5	18/3/5	24/0/2	20/4/2
Avg	g. rank	2.26	9.27	2.92	7.35	4.54	8.92	4.31	11.35	5.96	6.08	8.42	4.81
Over	all rank	1	11	2	8	4	10	3	12	6	7	9	5

Note: The optimal values are highlighted in bold.

Table 4. A comparison of the best fitness values between IVYPSO and 10 other algorithms for various test functions.

Func.	Metrics	IVYPSO	PSO	IVY	BOA	WOA	GOOSE	HPSOBOA	dFDB_LSHADE	FDC_AGDE	NSM_BO	dFDB_SFS	FDB_AGSK
F1	Best	0	1.9195 10	3.2648×10^{-260}	7.6243×10^{-11}	2.3137×10^{-83}	0.0134	2.2327×10^{-291}	6221.6016 12	0.0075 8	3.9426×10^{-5}	26.8336 11	3.2275×10^{-104}
F2	Rank Best	0	4.8081	0	2.4927×10^{-08}	3.6914×10^{-49}	12.8456	7.8194×10^{-146}	32.7774	0.0182	0.0051	5.3565	5.2776×10^{-63}
F3	Rank Best	1 0	9 53.1933	$ \begin{array}{c} 1\\6.5785 \times 10^{-95} \end{array} $	65.085×10^{-11}	5 428.7845	11 0.7136	3 2.9839 \times 10 ⁻²⁹²	12 169.5741	8 4.42	7 1.3085	10 161.3353	4 724.5566
F4	Rank	1	8 1.8277	3 0	4	11	5 0.3557	2	10 2.9046	7 1.4183	6	9 1.0204	12 8.0432
	Best Rank	1	9	ĭ	$2.466 \times 10^{-08} $ 4	0.4163 6	5	5.2086×10^{-147}	11	8	2.6106 10	7	12
F5	Best Rank	0.2523 8	0.9559 10	0.6904	5.1787 11	0.0725 5	0.007 3	0.0302 4	39.4716 12	5.2662×10^{-5}	3.4297×10^{-5}	0.2432 7	0.136 6
F6	Best	1.1454×10^{-5}	45.8573	3.2954×10^{-5}	0.0014	0.0011	0.1351	5.385×10^{-5}	2.6236	0.066 7	0.1496	0.0931	1.2591×10^{-5}
F7	Rank Best	$\frac{2}{3.1914 \times 10^{-19}}$	12 0	6.3819×10^{-35}		5 7.1751×10^{-66}	99.334×10^{-66}	4 1.7703×10^{-62}	$\begin{array}{c} 11 \\ 8.2727 \times 10^{-52} \end{array}$	7.1751×10^{-66}	$\begin{array}{c} 10 \\ 7.1751 \times 10^{-66} \end{array}$	$ 8 \\ 1.1911 \times 10^{-65} $	3 7.1751×10^{-66}
F8	Rank Best	11 0	1 0.3335	10 0	$12 \\ 1.1492 \times 10^{-13}$	$2 \\ 2.5197 \times 10^{-100}$	68.3454×10^{-6}	8 1.7958×10^{-295}	9 1.4189×10^{-5}	2 4.3298×10^{-21}	$2 \\ 1.2446 \times 10^{-23}$	7 9.3771×10^{-11}	2 7.2831 \times 10 ⁻¹⁵²
	Rank	1	12	1	8	5	10	3	11	7	6	9	4
F9	Best Rank	0 1	25.8431 11	4.3686×10^{-95}	7.5806×10^{-11}	1.2833×10^{-82} 5	0.7984 9	2.2617×10^{-291}	545.8044 12	0.0003 8	0.0003 7	4.3525 10	2.3672×10^{-106}
F10	Best Rank	27.0059 1	673.4298 11	27.899 3	28.9468 6	27.7308 2	30.1997 8	28.8365 5	21,955.7713 12	29.2534 7	396.3681 10	203.3141 9	28.7384 4
F11	Best	0 1	85.9941 11	0	6.8182×10^{-11}	3.5927×10^{-81} 5	0.244 9	1.9516×10^{-291}	894.8034 12	0.0007 8	1.665×10^{-5}	0.9829 10	1.1737×10^{-108}
F12	Rank Best	0.6667	222.886	0.66667	6 0.9 <u>6</u> 32	0.6667	0.8154	0.9953	2331.6115	0.7225	6.9031	4.5096	0.6774
F13	Rank Best	1 0	$\begin{array}{c} 11 \\ 2.0826 \times 10^{-27} \end{array}$	0	7 5.5035×10^{-26}	0	6 0.0017	8 0.0598	12 0.0089	5 4.8456×10^{-42}	10 0	9 2.4964×10^{-33}	0
F14	Rank Best	1	8 7.0078×10^{-22}	1	9 7.8597×10^{-20}	$\begin{array}{c} 1\\ 5.0035 \times 10^{-125} \end{array}$	10 0.013	12 0.0256	11 0.5158	6 5.1081×10^{-27}	1	7 1.1492×10^{-19}	$1 \\ 1.0275 \times 10^{-152}$
F15	Rank Best	1	7	18.3154×10^{-262}	8	5.0003×10^{-10} 5 4.1221×10^{-133}	10 0.0004	11	12 0.0002	6	1	9	4
	Rank	1	1.1273×10^{-30}	4	$5.7109 \times 10^{-22} \\ 10$	6	12	1.9605×10^{-296}	11	2.3713×10^{-40} 7	1	2.0643×10^{-31}	$1.7744 \times 10^{-188} \\ 5$
F16	Best Rank	0 1	207.2783 11	0 1	2.8422×10^{-13}	1.1369×10^{-13}	170.5284 9	0 1	227.4552 12	45.5111 8	6.967 7	197.8528 10	0 1
F17	Best Rank	0	174.921 9	0	167.5903 8	0	280.0004 12	0	217.8745 11	35.3575 7	6.0006	206.6572 10	0
F18	Best	4.4409×10^{-16}	2.8075	4.4409×10^{-16}	2.5252×10^{-8}	4.4409×10^{-16}	0.0649	4.4409×10^{-16}	9.5098	0.0115	0.9373	2.0932	3.9968×10^{-15}
F19	Rank Best	1 0	11 0.1039	1 0	$6 \\ 1.8527 \times 10^{-11}$	1 0	8 289.0103	0	12 57.1856	7 0.0152	9 0.1684	10 1.1599	0
F20	Rank Best	1	8 2.3272	1 0		$\begin{array}{c} 1 \\ 2.1642 \times 10^{-50} \end{array}$	12 8.4344	$\begin{array}{c} 1 \\ 6.1344 \times 10^{-147} \end{array}$	11 23.0176	7 0.0272	9 0.0005	10 8.9652	$1\\1.3616\times 10^{-67}$
	Rank	1	9	1	6	5	10	3	12	8	7 _	11	4
F21	Best Rank	0.0068 4	0.0125 6	0.0198 8	0.4861 10	0.0181 7	3.3439 12	0.0013 3	3.2316 11	4.0407×10^{-6}	2.7412×10^{-7} 1	0.0211 9	0.0107 5
F22	Best Rank	2.9661 10	0.8753 8	2.9715 11	2.9968 12	0.0595 5	0.0147 3	0.0651 6	1.5015 9	2.0754×10^{-6}	7.3649×10^{-9}	0.052 4	0.2135 7
F23	Best	0.0134	5.2542	2.1048	6.4945	0.3179	0.2986	1.5223 7	5.6278	0.051	1.235	1.6193	0.0021
F24	Rank Best	2 0	10 3.2678	0	12 0	5 0	4 2.0776	0	11 38.2506	3 0	6	8 0	1 0
F25	Rank Best	1 0	11 2.4874	1 0	1 0.8955	1 0.398	10 1.5919	1 0.0995	12 25.468	1 0.8955	1 6.3676	1 0.9069	1 0.0995
F26	Rank Best	1	10 14.0908	1	7 7.6919×10^{-11}	5 0	9 5.3631	4 0	12 54.1892	6 0.0006	11 0.0253	8 3.8484	3
	Rank	1	11	1	7.0919 × 10 6	1	10	1	12	7	8	9	1
Avg.	Paired rank + rank	/=/- 2.19	24/0/2 9.35	9/15/2 3.08	25/0/1 7.27	16/7/3 4.08	23/0/3 8.5	16/6/4 3.92	24/0/2 11.35	21/1/4 5.92	18/4/4 5.85	22/1/3 8.46	16/6/4 3.92
Overal	ll rank	1	10	2	8	5	10	3	11	7	6	9	3

Note: The optimal values are highlighted in bold.

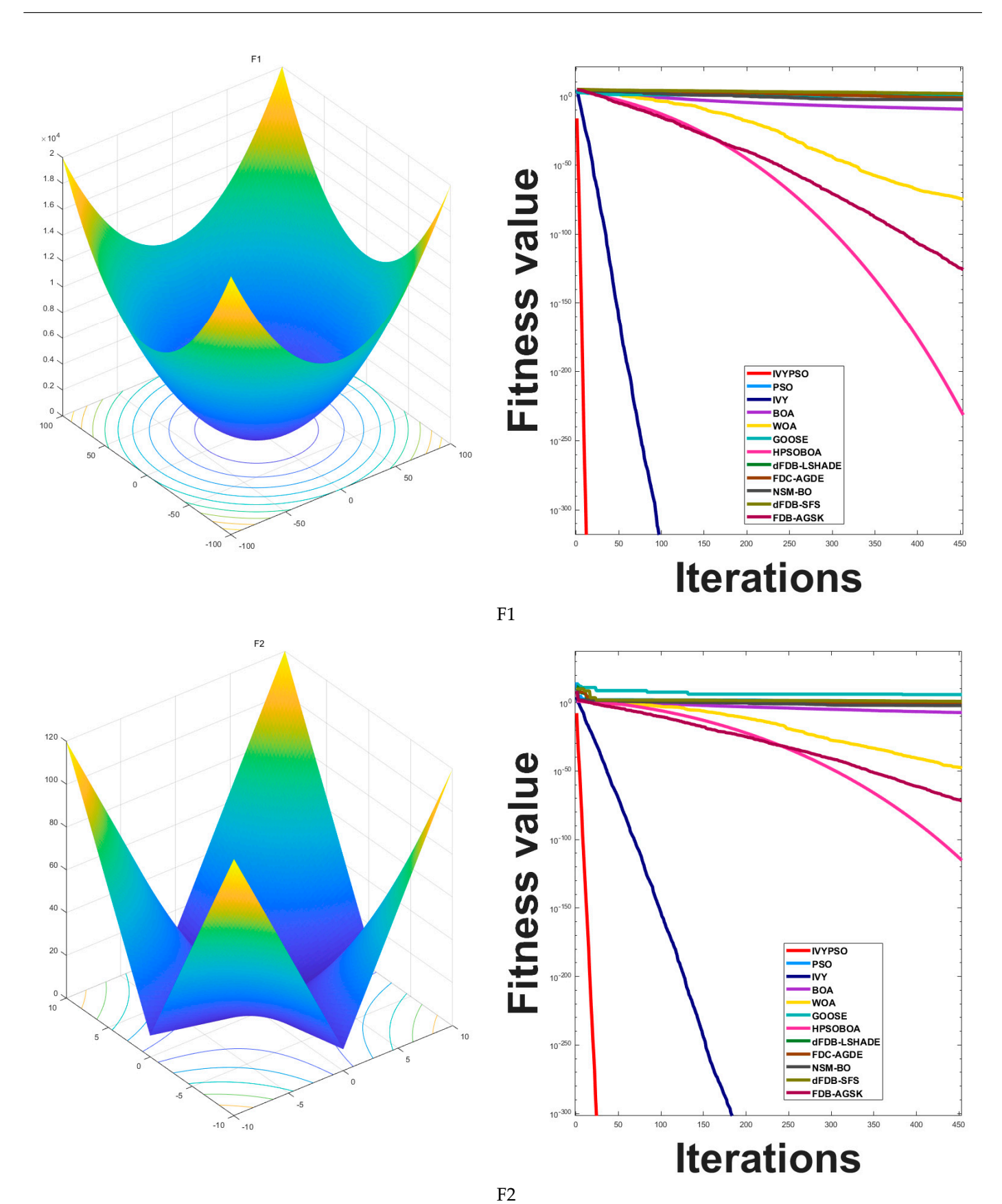


Figure 5. Cont.

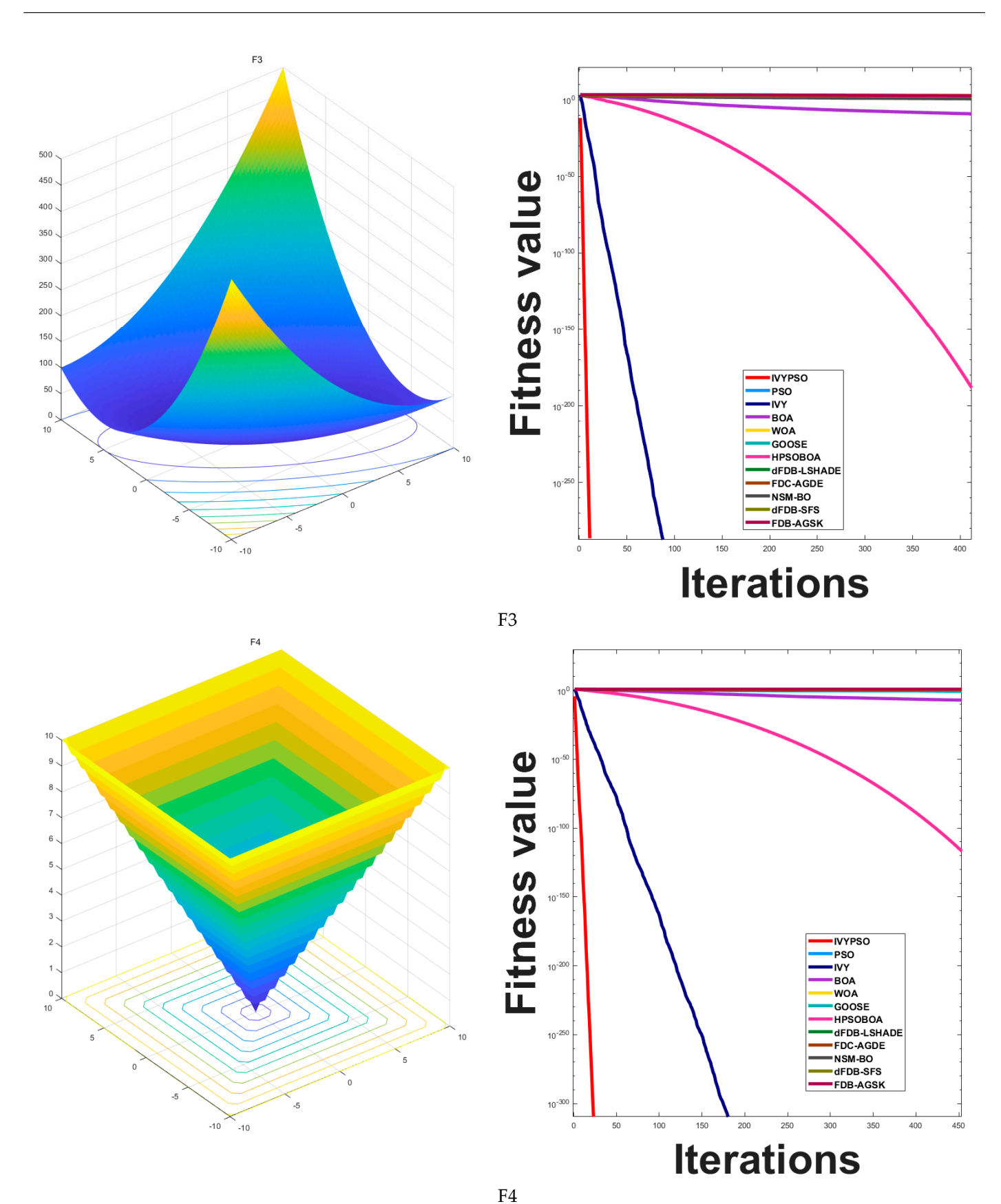


Figure 5. Cont.

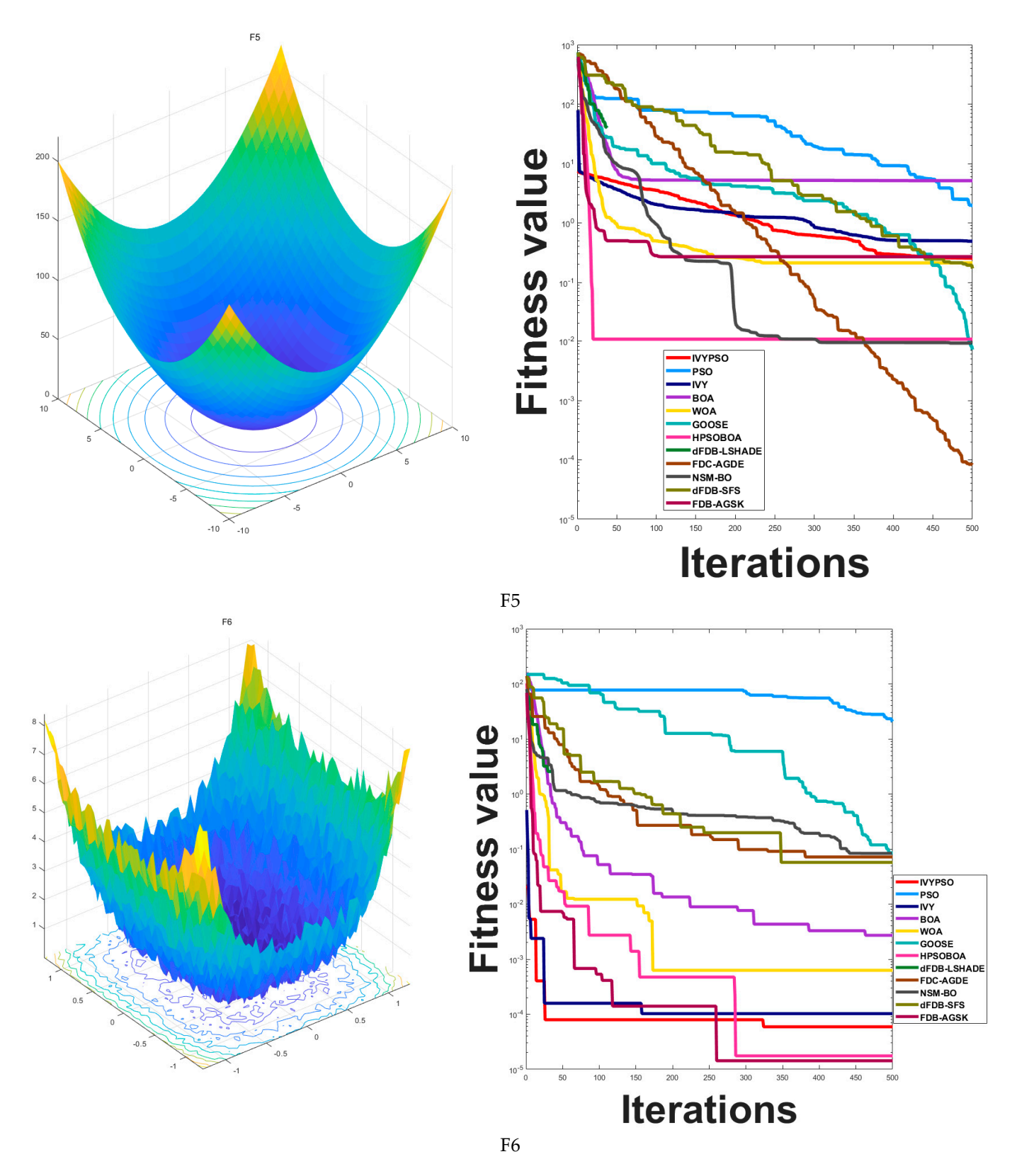


Figure 5. Cont.

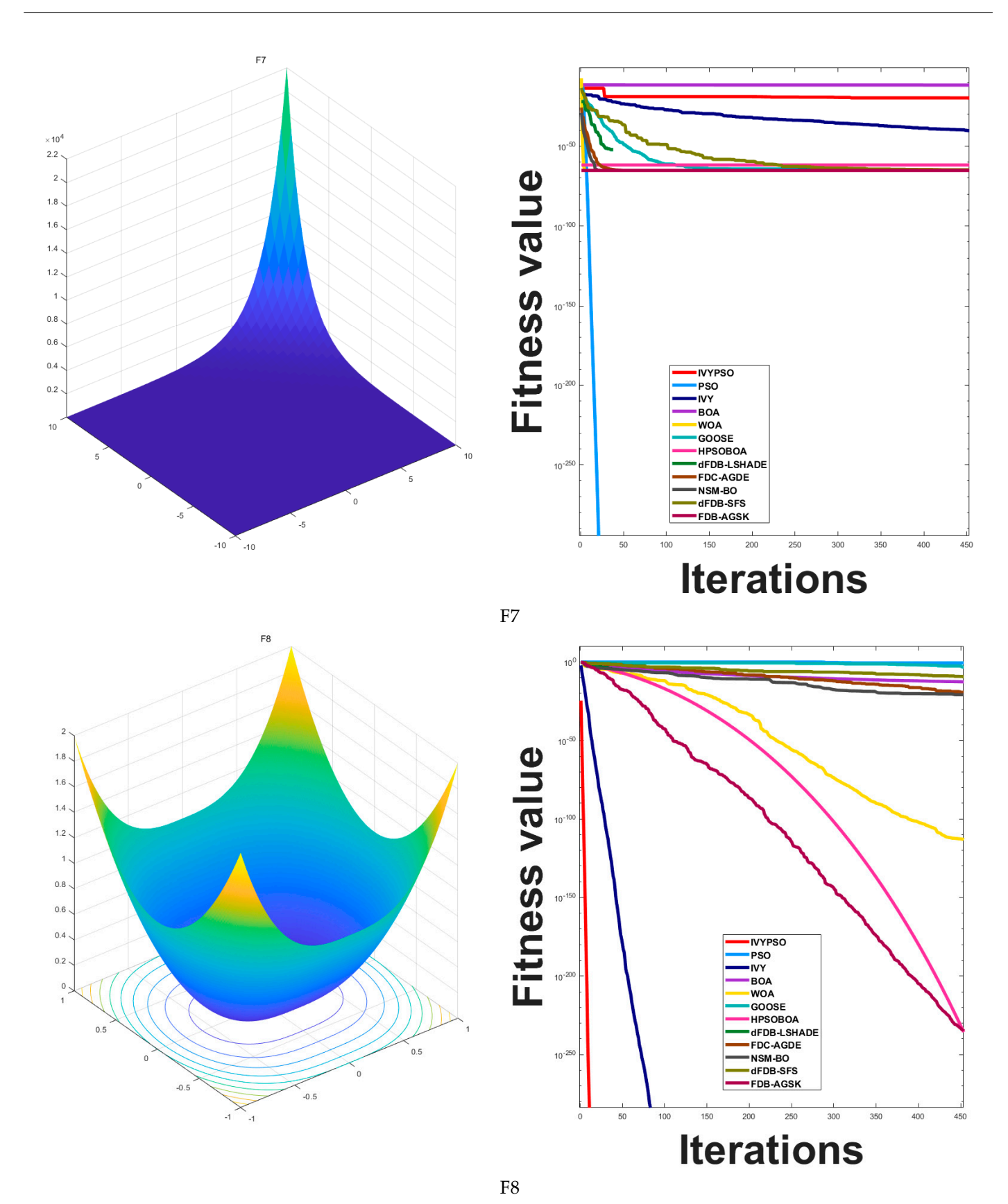


Figure 5. Cont.

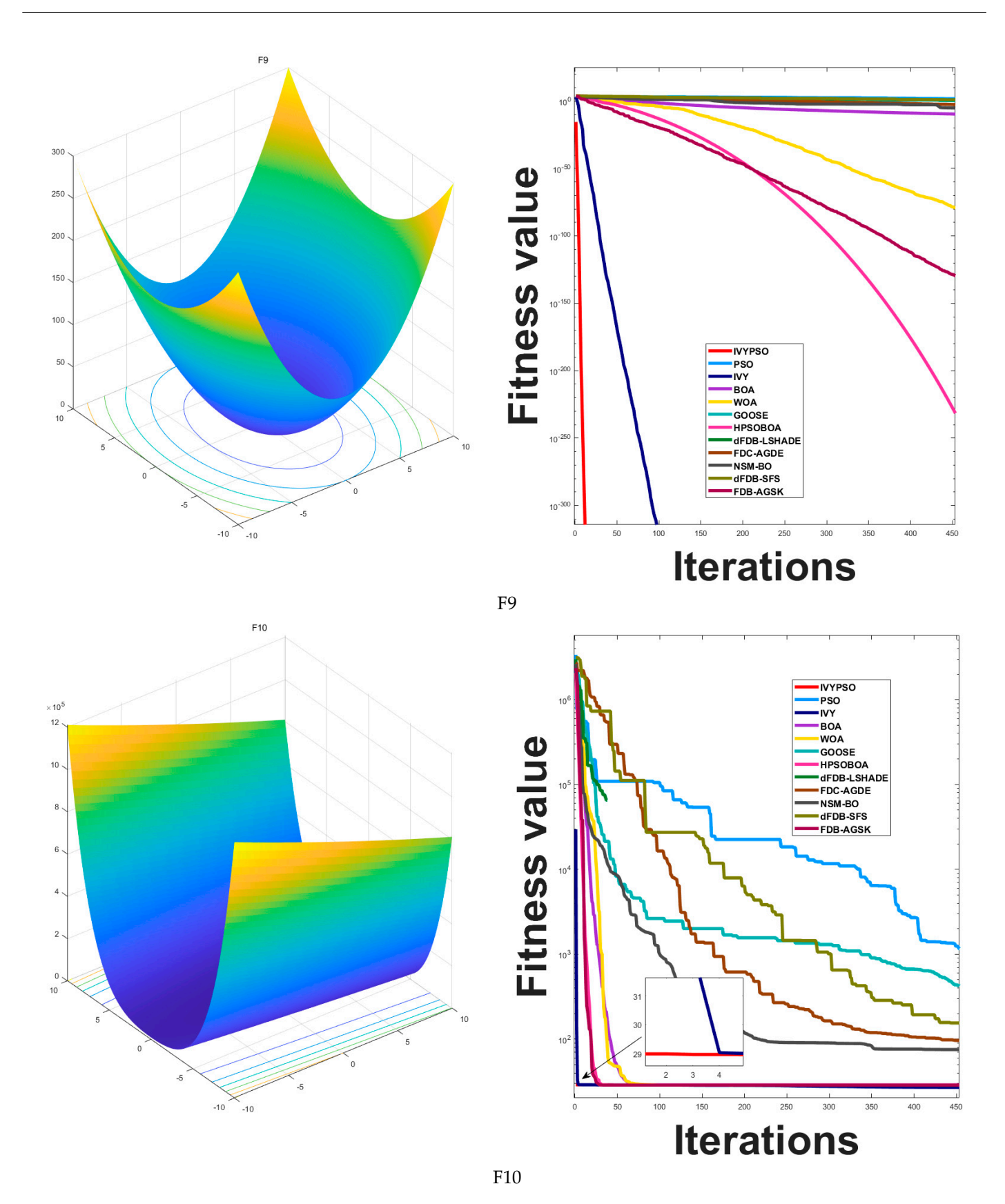


Figure 5. Cont.

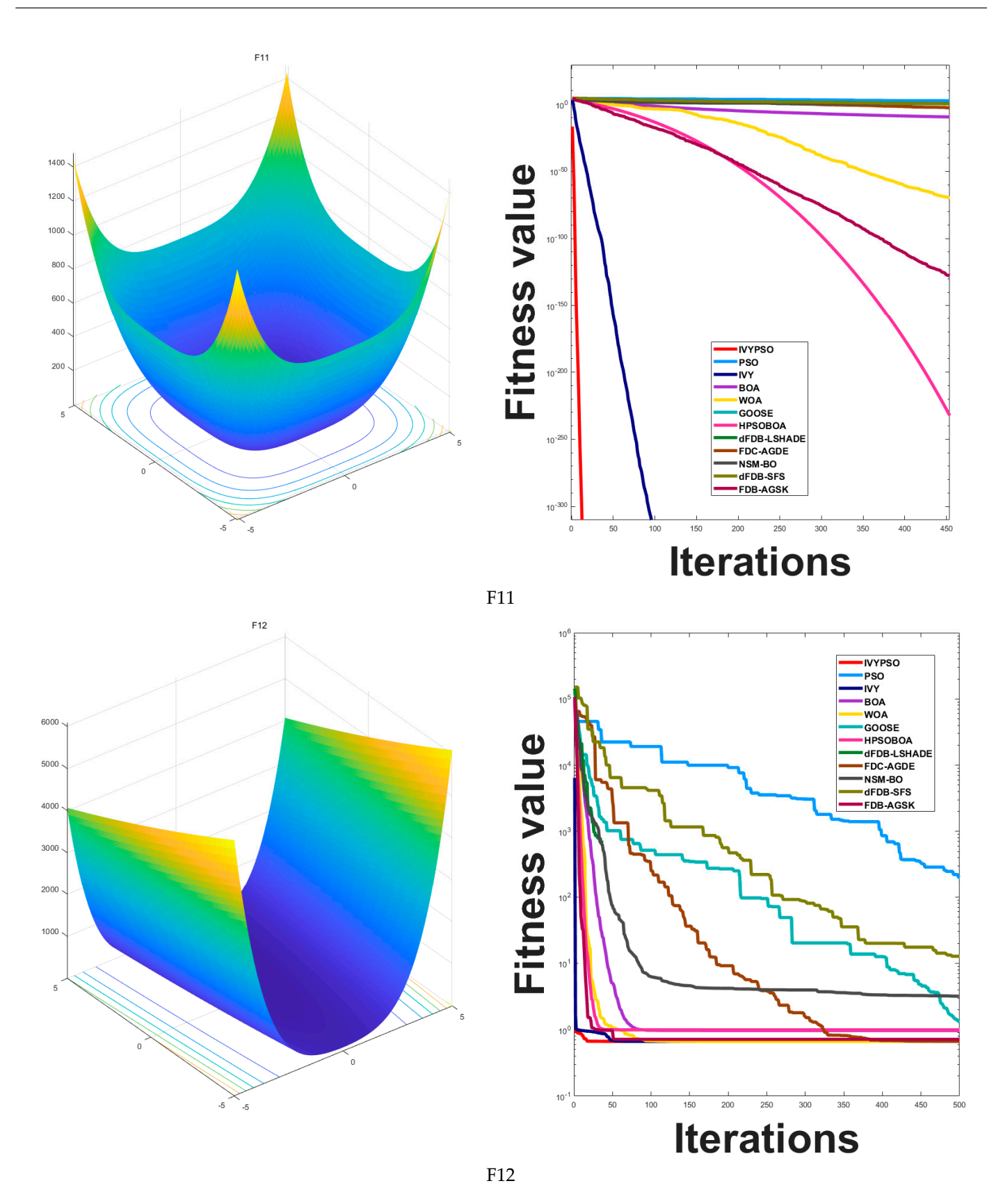


Figure 5. Cont.

Biomimetics **2025**, 10, 342 25 of 41

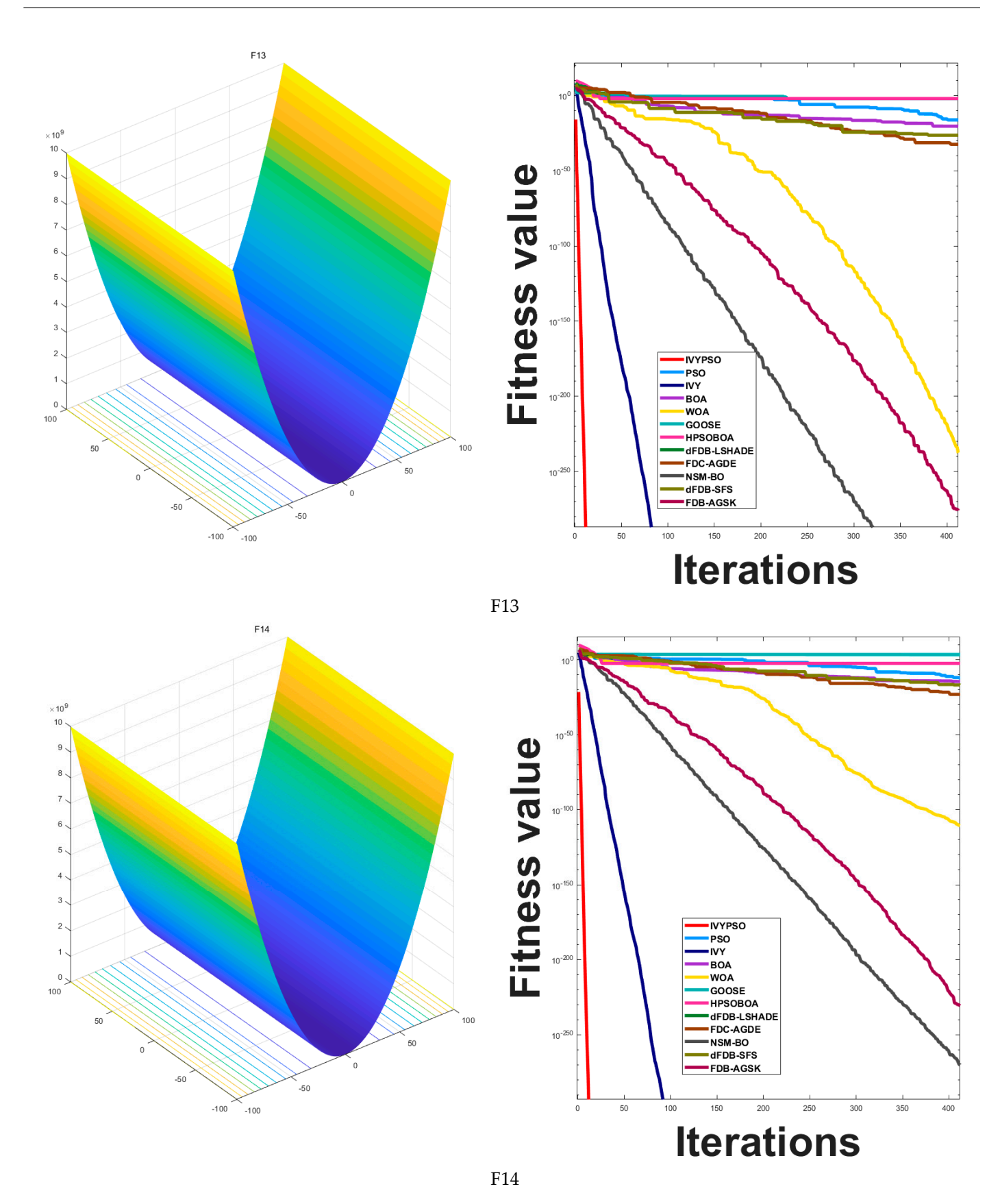


Figure 5. Cont.

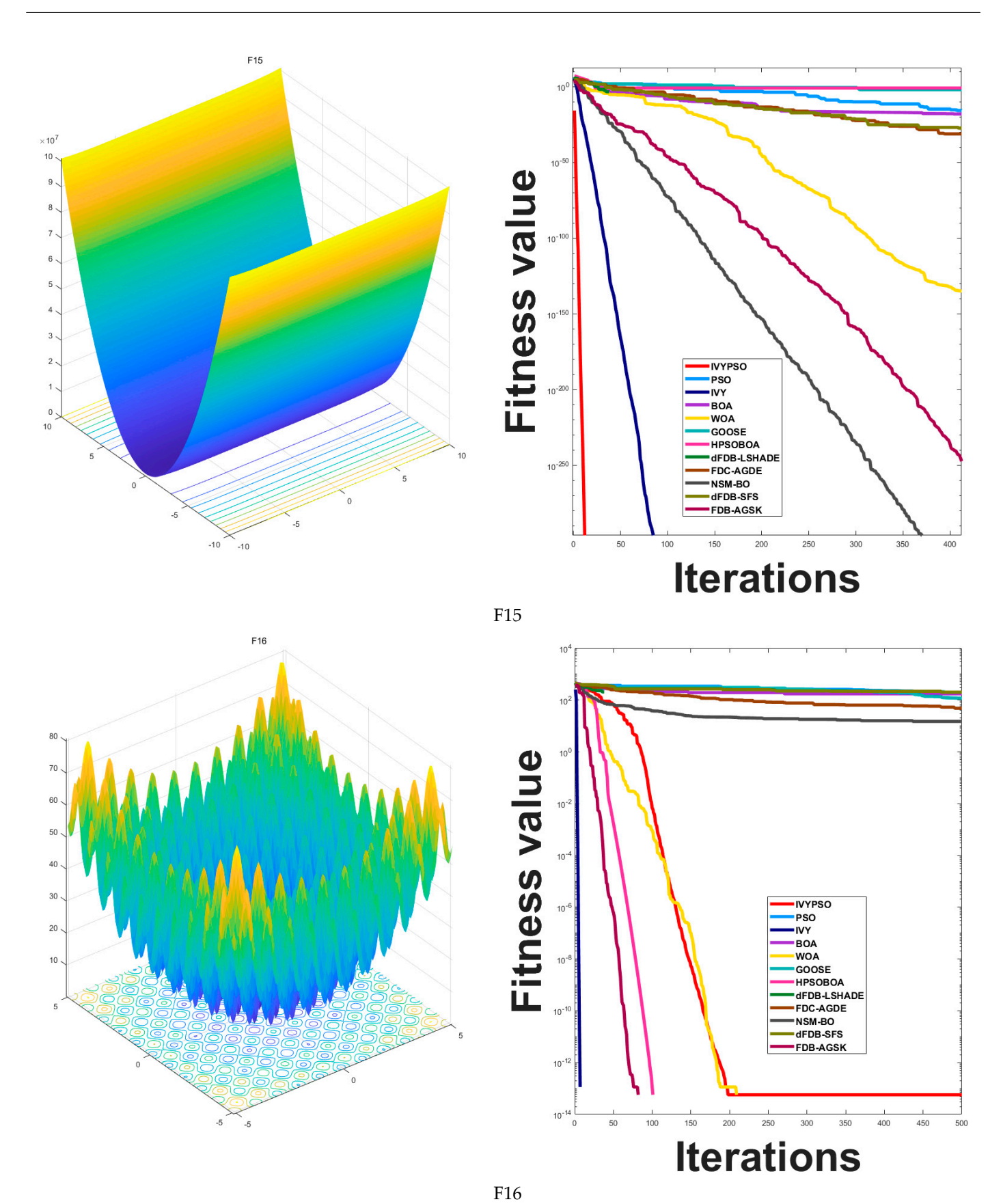


Figure 5. Cont.

Biomimetics **2025**, 10, 342 27 of 41

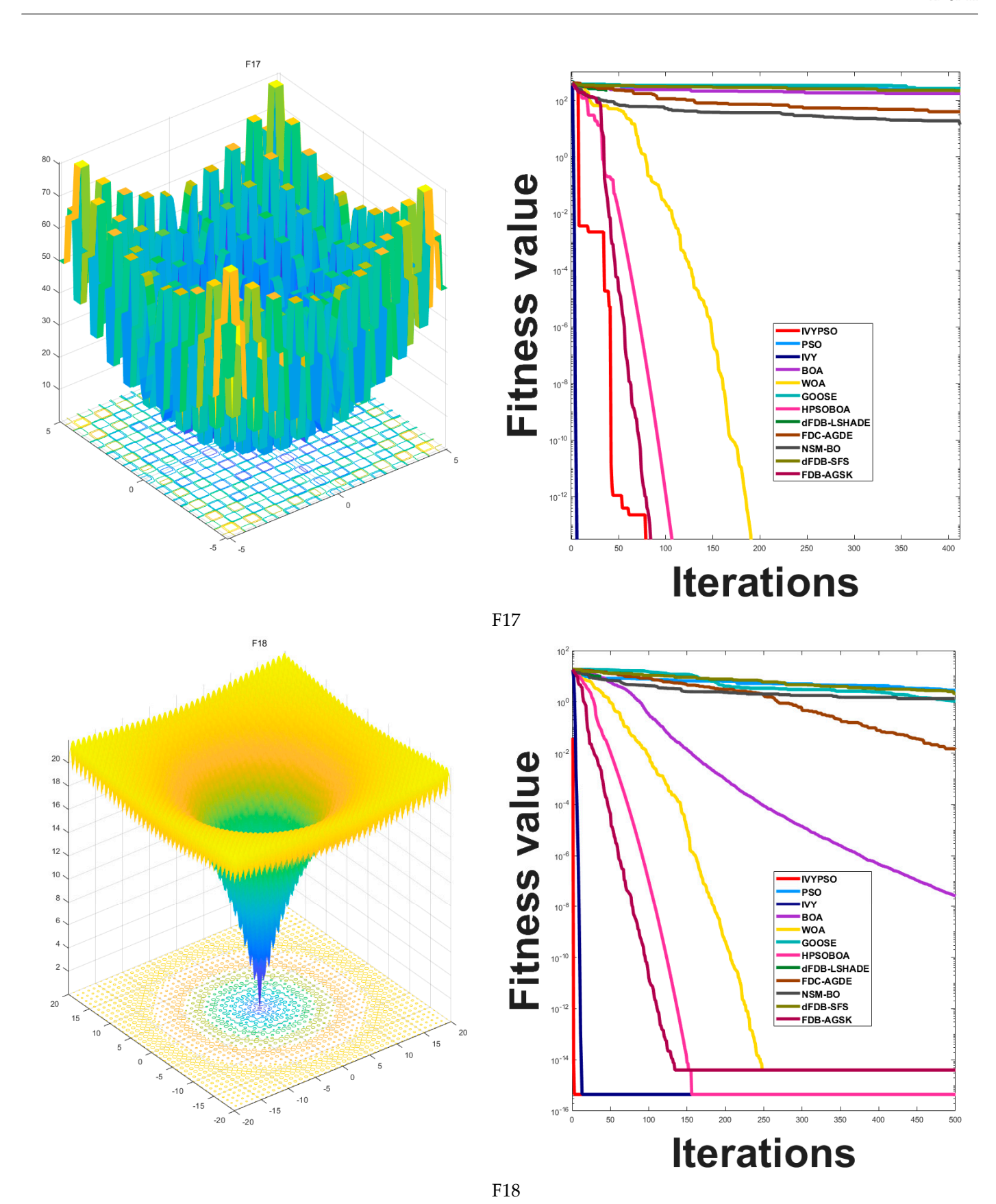


Figure 5. Cont.

Biomimetics **2025**, 10, 342 28 of 41

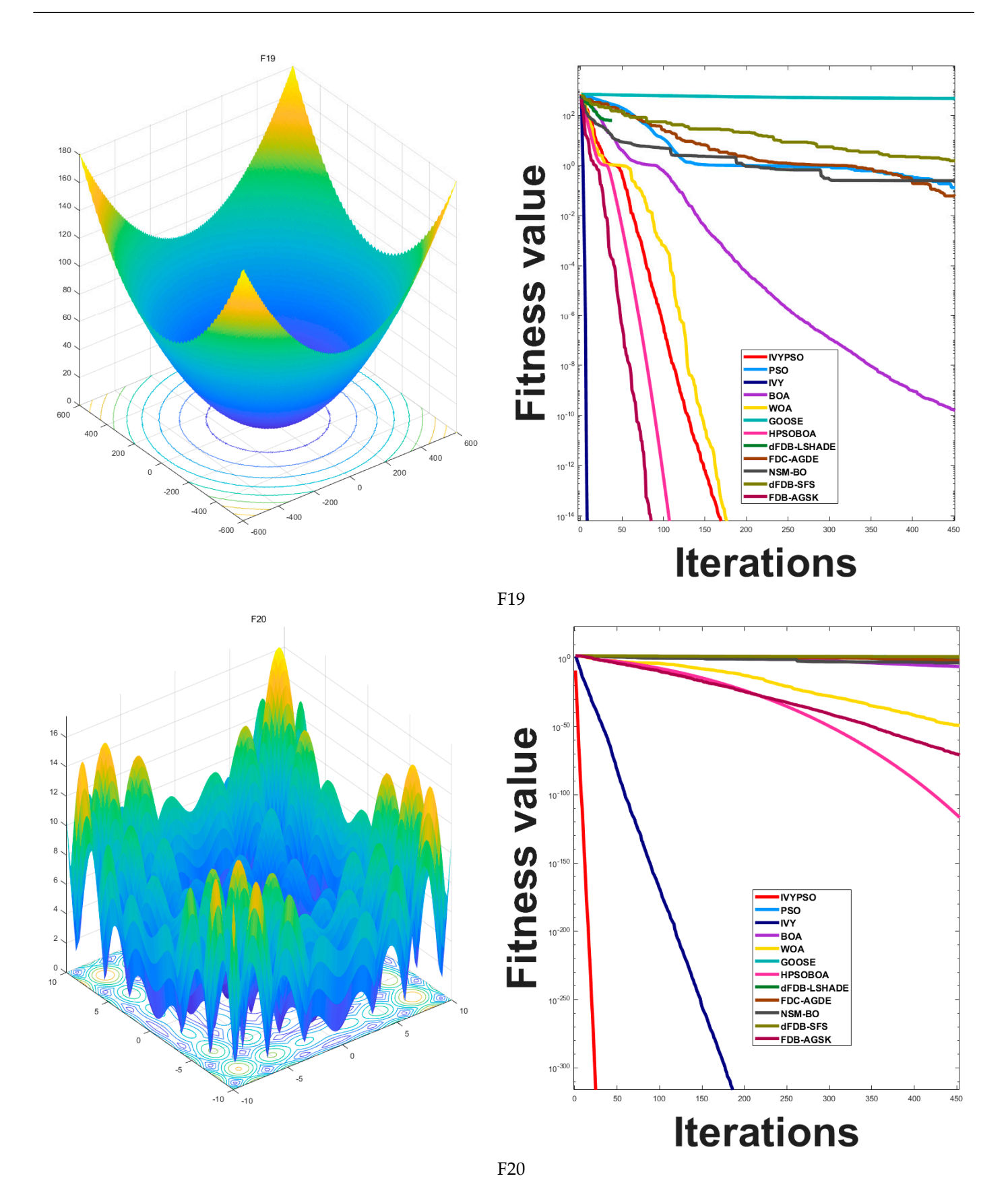


Figure 5. Cont.

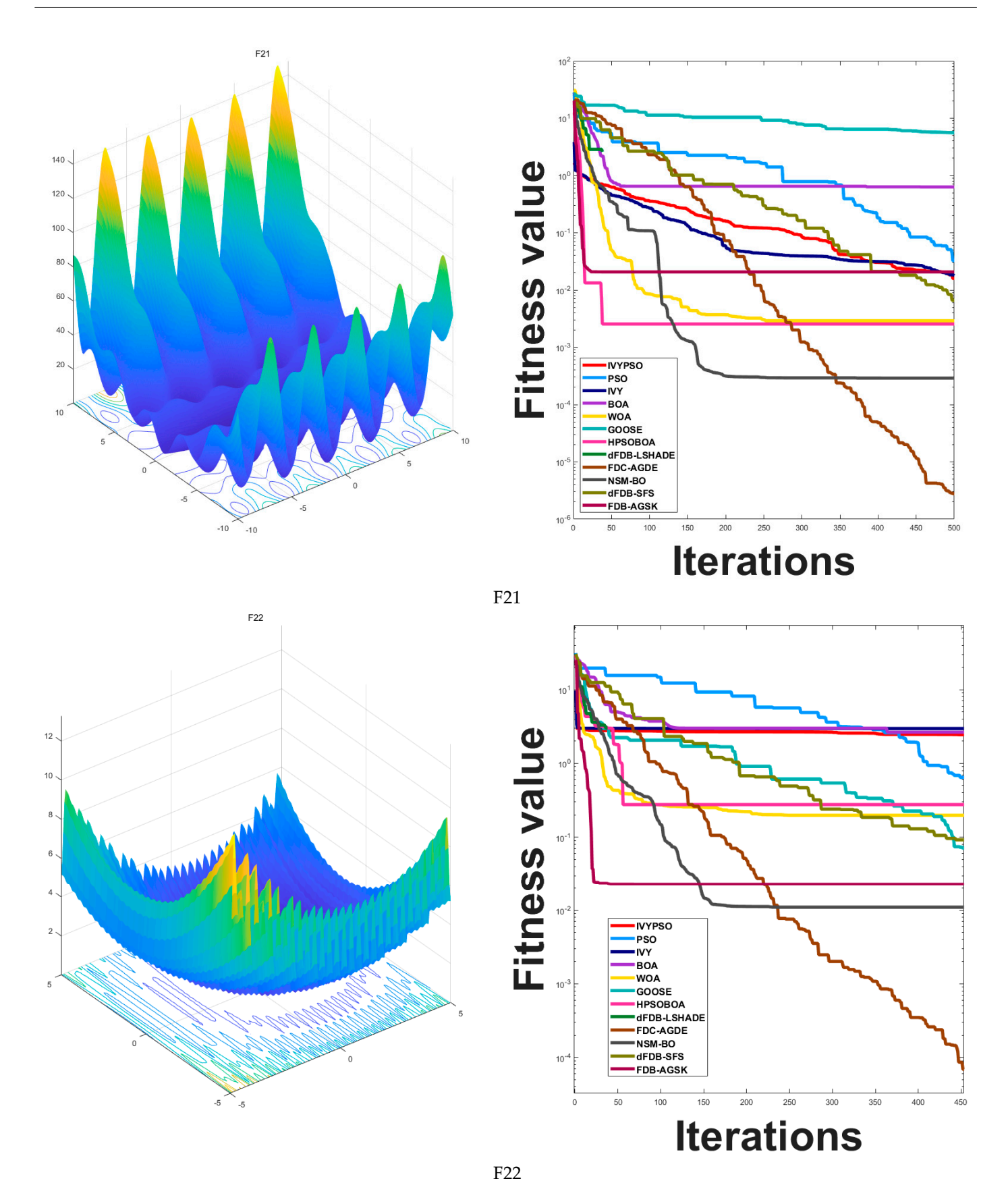


Figure 5. Cont.

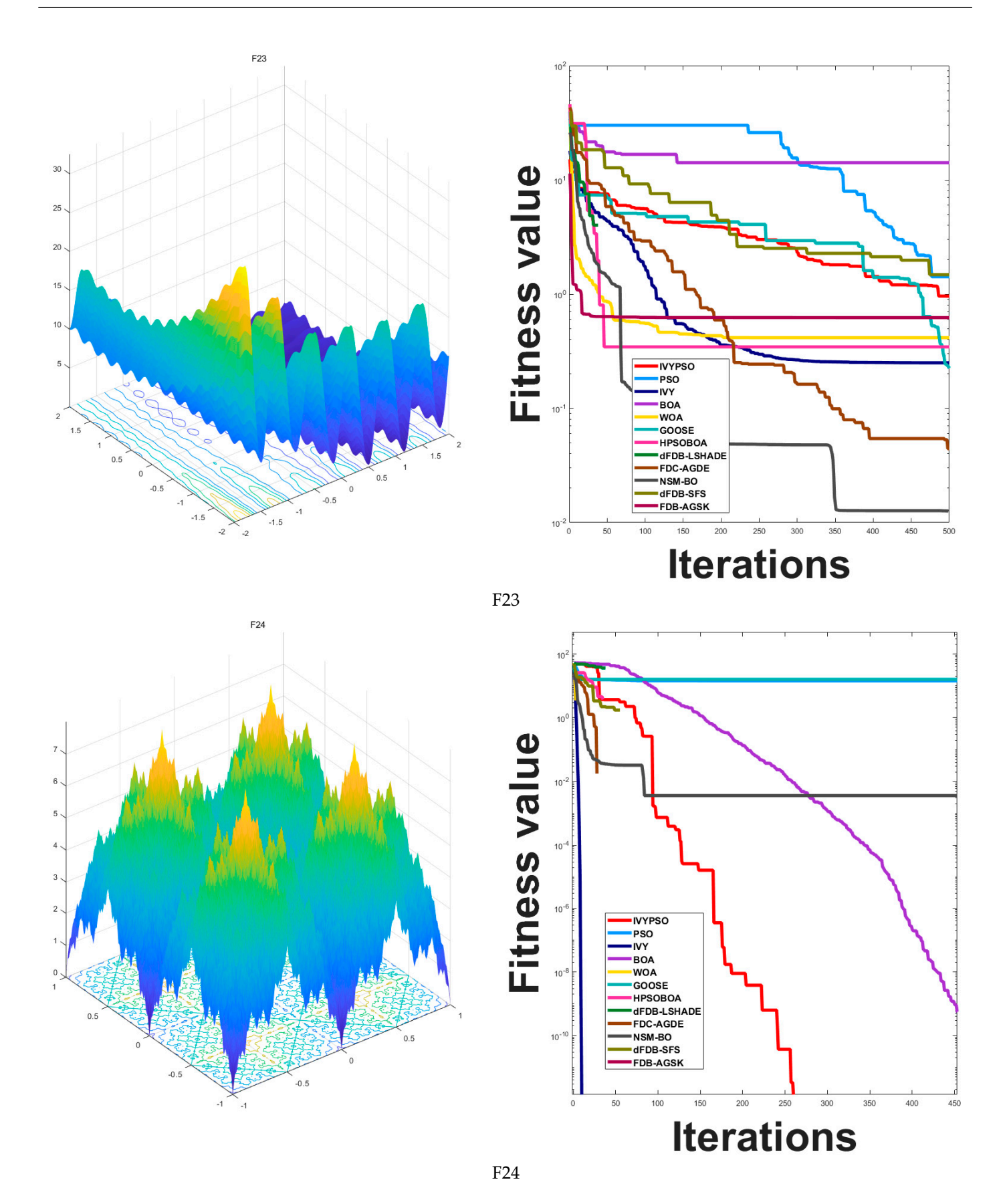


Figure 5. Cont.

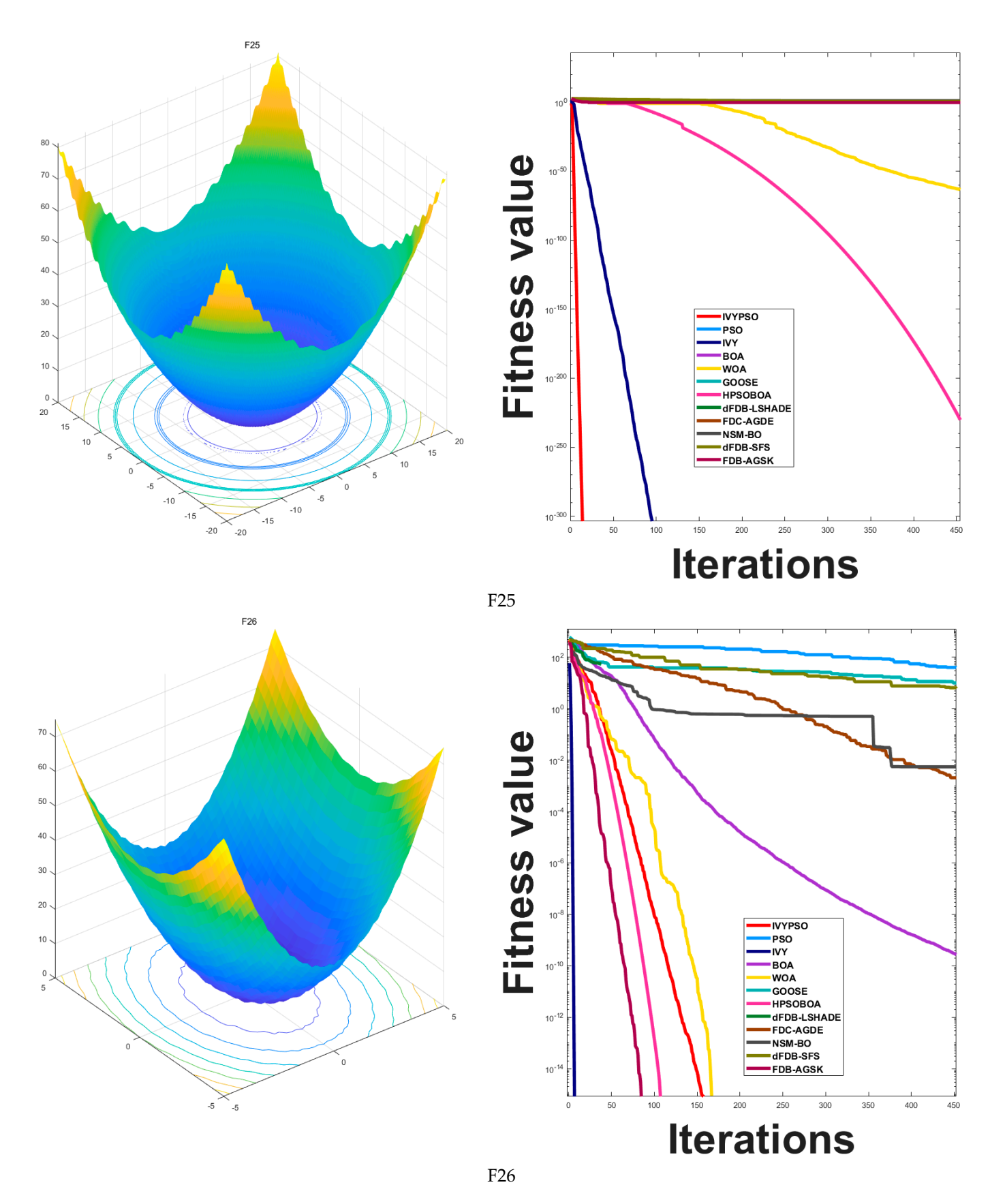


Figure 5. The convergence behaviors of IVYPSO and other algorithms for various test functions.

Biomimetics **2025**, 10, 342 32 of 41

Tr. f	-1- F D	14 6-41	TA7:1		1	toot from alians	:-: tl: 0.0E
Iai	bie 5. Kesu	its of the	vviicoxon	signed-ran	k test for 26	test functions	s with $\alpha = 0.05$.

Algorthm	Wilcoxon Test <i>p</i> -Value	Significant
IVYPSO-PSO	2.4153×10^{-5}	Yes
IVYPSO-IVY	1.6357×10^{-2}	Yes
IVYPSO-BOA	2.9991×10^{-5}	Yes
IVYPSO-WOA	4.5685×10^{-2}	Yes
IVYPSO-GOOSE	5.0978×10^{-5}	Yes
IVYPSO-HPSOBOA	1.6067×10^{-2}	Yes
IVYPSO-FDC-AGDE	8.3166×10^{-3}	Yes
IVYPSO-dFDB-LSHADE	7.8847×10^{-6}	Yes
IVYPSO-NSM-BO	3.8919×10^{-3}	Yes
IVYPSO-dFDB-SFS	5.9619×10^{-5}	Yes
IVYPSO-FDB-AGSK	1.5664×10^{-3}	Yes

To evaluate further the overall performance of the proposed IVYPSO algorithm on the 26 benchmark functions, the Friedman scores were used to rank the average performances of 12 comparative algorithms [47–49]. Table 6 presents the Friedman scores and their corresponding ranks. Among all algorithms, IVYPSO achieved the lowest Friedman score of 1.9231, ranking first, which demonstrates its outstanding performance across all test functions. In contrast, traditional algorithms such as PSO and BOA obtained Friedman scores of 5.8846 and 6.7308, ranking 9th and 11th, respectively, indicating relatively weaker overall performance. Similarly, some improved algorithms, such as FDC-AGDE and dFDB-LSHADE, ranked 12th and 10th, respectively, also underperforming compared to IVYPSO. These results indicate that IVYPSO exhibits strong robustness and competitiveness in solving complex optimization problems, and its overall performance surpasses that of both traditional and newly developed metaheuristic algorithms.

Table 6. Friedman ranking scores of IVYPSO and other competing algorithms.

Friedman Scores	Rank
1.9231	1
5.8846	9
3.7308	2
6.7308	11
4.8462	3
5.4615	6
4.9615	4
7.0385	12
6.4231	10
5.4615	7
5.5385	8
5.0385	5
	1.9231 5.8846 3.7308 6.7308 4.8462 5.4615 4.9615 7.0385 6.4231 5.4615 5.5385

Note: The optimal values are highlighted in bold.

5.1.7. Analysis of Computational Expenses

The time complexity of the IVYPSO algorithm is primarily composed of three parts: the population initialization, iteration updates, and fitness evaluation. Let the population size be N, the maximum number of iterations be T, and the dimensionality of the decision variables be dim. In the population initialization phase, the random generation of each particle's position and velocity, along with the fitness evaluation, requires a time complexity of $O(N \times dim)$. In each iteration, the algorithm updates the velocity and position of each particle, adjusts the ivy growth variables, and evaluates the fitness. The velocity and position updates involve basic vector operations, with a time complexity of O(dim), and the ivy growth variable update and random perturbation for local or global searches also have a time complexity of O(dim). The fitness evaluation is usually the most time-

Biomimetics **2025**, 10, 342 33 of 41

consuming operation. If the complexity of the objective function evaluation is O(f), the fitness calculation for the entire population in each iteration has a time complexity of $O(N \times f)$. Therefore, the overall time complexity of the IVYPSO algorithm can be expressed as $O(T \times N \times (dim + f))$. As the population size N, maximum iteration count T, and dimensionality dim increase, the algorithm's time complexity grows linearly, making it suitable for large-scale, complex global optimization problems.

5.2. Application of IVYPSO to Engineering Optimization Problems

This section presents the application of the IVYPSO algorithm in solving engineering optimization problems that involve various inequality and equality constraints. For each optimization problem, IVYPSO was evaluated in 20 independent runs using a population size of 30 individuals, with a maximum of 500 iterations. The performance of IVYPSO was compared with 11 other algorithms, including PSO, IVY, BOA, WOA, GOOSE, HPSOBOA, FDC_AGDE, dFDB_LSHADE, NSM_BO, dFDB_SFS, and FDB_AGSK. Additionally, three stability analysis metrics were incorporated: SR, ACTs, and AFEs. SR represents the proportion of independent runs in which the algorithm successfully found solutions that satisfy all constraints and reach the global optimum or an acceptable level of precision. ACTs refers to the average time (in seconds) spent by the algorithm to complete each optimization task across multiple runs. AFEs indicates the average number of fitness function evaluations required to complete the optimization task over multiple experiments.

5.2.1. Gas Transmission Compressor Design (GTCD) Problem

Figure 6 illustrates the gas transmission compressor design (GTCD) problem, which is a representative and practical mechanical design case originally proposed by Beightler and Phillips [50]. This problem involves determining the optimal values of several design variables, such as the pipeline length, inlet and outlet pressures, and pipe diameter, with the objective of minimizing the total cost of a gas pipeline transmission system while ensuring the delivery of 100 million cubic feet of natural gas per day.

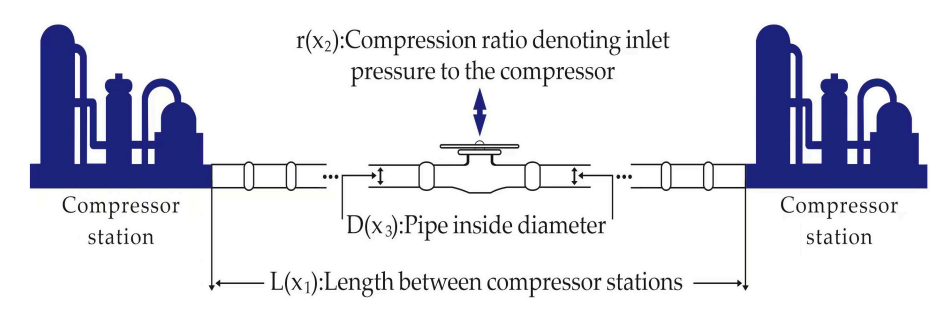


Figure 6. A gas pipeline transmission system for the GTCD problem.

The GTCD problem reflects a realistic and complex engineering scenario widely encountered in energy and process industries. It poses significant optimization challenges due to its non-linear, constrained, and multimodal nature. By applying the proposed IVYPSO algorithm to this problem, we aim to demonstrate its capability to handle real-world design constraints, achieve cost-effective solutions, and maintain robustness in practical optimization tasks. This problem has three decision variables: the length L between two compressor stations; the compression ratio L, at the compressor inlet, where $r = \frac{P_1}{P_2}$, with P_1 being the pressure leaving the compressor station (psi) and P_2 being the pressure entering the compressor station (psi); and D, the internal diameter of the pipeline (inches). The goal is to find the optimal values for L, r, and D that minimize the C_1 value.

Biomimetics **2025**, 10, 342 34 of 41

In this problem, the total annual cost of the gas transmission system is defined as in Equation (24):

$$minC_{1}(x) = 8.61 \times 10^{5} x_{3}^{-\frac{2}{3}} x_{1}^{\frac{1}{2}} x_{2} (x_{2}^{2} - 1)^{-\frac{1}{2}}$$

$$+3.69 \times 10^{4} x_{3} - 7.6543 \times 10^{8} x_{1}^{-1}$$

$$+7.72 \times 10^{8} x_{1}^{-1} x_{2}^{0.219},$$
(24)

where $x_1 = L$, $x_2 = r$, $x_3 = D$, subject to:

$$10 \le x_1 \le 55$$
,

$$1.1 \le x_2 \le 2$$
,

$$10 \le x_3 \le 40$$
.

Table 7 presents a comparison of the results for solving the gas transmission compressor design problem using IVYPSO and other algorithms from the literature. The success rate threshold for this problem was determined to be 1,677,759.2755. The best result achieved by IVYPSO was L=24.4960, r=1.5867, D=20.0000, with a minimum cost of 1,677,759.2755 and with an SR value of 100%, which required minimal time to complete the task. Table 8 shows a statistical analysis, showing that IVYPSO achieved the lowest average cost of 1,677,759.2755. These results demonstrate that compared to other optimization algorithms, IVYPSO delivers a superior solution to the gas transmission compressor design problem.

Table 7. The best values obtained by IVYPSO and other competing algorithms for the GTCD problem.

Algorithm	L	r	D	Optimal Value	SR(%)	ACTs	AFEs
IVYPSO	24.496	1.5867	20	1,677,759.2755	100	0.1419	15,030
PSO	24.496	1.5867	20	1,677,759.2755	80	0.1187	15,030
IVY	24.496	1.5867	20	1,677,759.2755	80	0.172	15,030
BOA	20	1.1134	20	1,683,684.5457	0	0.1797	30,030
WOA	24.496	1.5867	20	1,677,759.2755	85	0.0938	15,000
GOOSE	32.5256	1.2305	20	1,677,759.2854	0	0.101	15,000
HPSOBOA	21	1.0537	21	1,685,732.6804	0	0.1786	30,030
FDC_AGDE	24.496	1.5867	20	1,677,759.2755	85	0.1087	15,030
dFDB LSHADE	28.5541	1.1932	20	1,677,783.3132	0	0.0047	500
NSM BO	24.496	1.5867	20	1,677,759.2755	100	0.3239	15,000
dFDB SFS	24.496	1.5867	20	1,677,759.2755	80	0.1978	15,000
FDB_AGSK	24.496	1.5867	20	1,677,759.2755	100	0.1845	15,000

Note: The optimal values are highlighted in bold.

Table 8. Statistical assessment of various algorithms applied to the GTCD problem.

Algorithm	Mean	Best	Worst	Median	Std	Rank
IVYPSO	1,677,759.2755	1,677,759.2755	1,677,759.2755	1,677,759.2755	0.0000	1
PSO	1,678,556.6157	1,677,759.2755	1,685,732.6774	1,677,759.2755	2521.4111	7
IVY	1,678,354.4837	1,677,759.2755	1,685,634.2755	1,677,759.2755	1932.6400	6
BOA	1,685,527.8813	1,683,684.5457	1,685,732.7254	1,685,732.6942	647.6821	8
WOA	1,677,759.2760	1,677,759.2755	1,677,759.2777	1,677,759.2756	0.0009	4
GOOSE	2,048,858.2698	1,677,759.2854	5,177,439.6140	1,698,815.7980	1,099,516.1908	12
HPSOBOA	1,685,748.4393	1,685,732.6804	1,685,810.0629	1,685,735.5707	25.3056	9
FDC_AGDE	1,778,373.1947	1,677,759.2755	2,675,925.0653	1,677,759.2755	315,377.5360	11
dFDB_LSHADE	1,678,255.5734	1,677,783.3132	1,679,765.5234	1,678,075.9952	619.2305	5
NSM_BO	1,677,759.2755	1,677,759.2755	1,677,759.2755	1,677,759.2755	0	1
dFDB_SFS	1,694,760.8055	1,677,759.2755	1,762,766.9254	1,677,759.2755	35,842.3723	10
FDB_AGSK	1,677,759.2755	1,677,759.2755	1,677,759.2755	1,677,759.2755	0	1

Note: The optimal values are highlighted in bold.

5.2.2. Three-Bar Truss Design Problem

Figure 7 shows the three-bar truss design problem. The three-bar truss is typically a simple planar truss structure composed of three rods forming a triangular shape. This

Biomimetics **2025**, 10, 342 35 of 41

problem is widely applicable in engineering design, particularly in the field of structural optimization. The design variables typically include the cross-sectional area or dimensions of the rods, with the objective of minimizing the total mass of the truss while ensuring compliance with stress and geometric constraints. Such problems effectively reflect real-world engineering demands for structural safety and material efficiency, making them commonly used as benchmark problems for evaluating the performance of optimization algorithms.

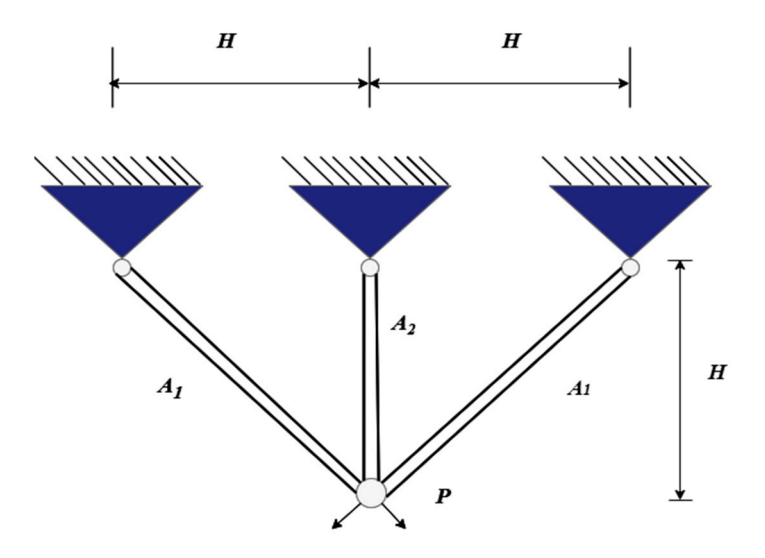


Figure 7. Schematic diagram of the three-bar truss design.

The total mass of the three-bar truss can be expressed by Equation (25):

$$\min f(x) = \left(2\sqrt{2}x_1 + x_2\right) \times H \tag{25}$$

where $x_1 = A_1$, $x_2 = A_2$:

$$g_1(x) = \frac{\sqrt{2}x_1 + x_2}{\sqrt{2}x_1 + \frac{2x_1x_2}{x_2}}P - \sigma \le 0,$$

$$g_2(x) = \frac{P}{\sqrt{2}x_1 + \frac{2x_1x_2}{x_2}} - \sigma \le 0,$$

$$g_3(x) = \frac{P}{x_1 + \sqrt{2}x_2} - \sigma \le 0,$$

 $0 \le x_1, x_2 \le 1.$

where H = 1000 mm, P = 2 kN/cm^2 , $\sigma = 2 \text{ kN/cm}^2$.

Table 9 presents a comparison of the results for solving the three-bar truss design problem using IVYPSO and other algorithms from the literature. The success rate threshold for this problem was determined to be 263.8523. The best result obtained by IVYPSO was $A_1=0.7884,\,A_2=0.4081,\,$ with a minimum cost of 263.8523 and an SR value of 100%, and it required minimal time to complete the task. Table 10 provides a statistical analysis, showing that IVYPSO achieved the lowest average cost of 263.8523. These results indicate that compared to other optimization algorithms, IVYPSO provides a better solution for the three-bar truss design problem.

Biomimetics **2025**, 10, 342 36 of 41

Algorithm	X1	X2	Optimal Value	SR (%)	ACTs	AFEs
IVYPSO	0.7884	0.4081	263.8523	100	0.1531	15,030
PSO	0.7884	0.4081	263.8523	85	0.1663	15,030
IVY	0.7884	0.4081	263.8523	90	0.2151	15,030
BOA	0.7937	0.3938	263.8849	0	0.2743	30,030
WOA	0.7919	0.3984	263.8611	0	0.137	15,000
GOOSE	0.7884	0.4081	263.8523	100	0.1447	15,000
HPSOBOA	0.8374	0.4669	264.2474	0	0.2783	30,030
FDC AGDE	0.7884	0.4081	263.8523	100	0.1518	15,030
dfdb Lshade	0.7884	0.4081	263.8523	90	0.0058	500
NSM_BO	0.7884	0.4081	263.8523	100	0.357	15,000
dFDB SFS	0.7884	0.4081	263.8523	100	0.2654	15,000
						'

263.8523

Table 9. The best values obtained by IVYPSO and other competing algorithms for the three-bar truss design problem.

Note: The optimal values are highlighted in bold.

0.4081

FDB AGSK

0.7884

Table 10. Statistical assessment of various algorithms applied to the three-bar truss design problem.

100

0.2167

15,000

Algorithm	Mean	Best	Worst	Median	Std	Rank
IVYPSO	263.8523	263.8523	263.8523	263.8523	0	1
PSO	263.9375	263.8523	264.7016	263.8523	0.2685	9
IVY	263.8524	263.8523	263.8527	263.8524	6.97×10^{-4}	7
BOA	264.1555	263.8787	264.8682	264.0228	0.3227	10
WOA	265.3408	263.8591	268.7184	264.7459	1.8316	11
GOOSE	263.8524	263.8523	264.5934	263.8523	0.2397	6
HPSOBOA	271.5462	264.4945	279.0356	272.9894	4.4763	12
FDC_AGDE	263.8523	263.8523	263.8523	263.8523	0	1
dFDB_LSHADE	263.8573	263.8524	263.8955	263.8527	0.0134	8
NSM_BO	263.8523	263.8523	263.8523	263.8523	0	1
dFDB_SFS	263.8523	263.8523	263.8523	263.8523	0	1
FDB_AGSK	263.8523	263.8523	263.8523	263.8523	0	1

Note: The optimal values are highlighted in bold.

5.2.3. Multiple-Disk Clutch Brake Design Problem

Figure 8 illustrates the multiple-disk clutch brake design problem, a classic engineering optimization issue that is commonly encountered in automation equipment, mechanical transmission systems, and the automotive industry [51]. This problem involves optimizing the design of the clutch and brake system to minimize the stopping time of the brake while ensuring high operational efficiency and stability. Such design problems are highly relevant to real-world engineering scenarios, where the balance between performance, efficiency, and reliability is critical. By addressing this problem, the algorithm's ability to handle practical engineering challenges and improve the overall system design is demonstrated, reflecting its applicability in real-world applications. This problem involves five decision variables: the inner radius \mathbf{r}_i in millimeters, outer radius \mathbf{r}_o in millimeters, disk thickness t in millimeters, driving force F, and number of friction surfaces Z.

The brake's stopping time can be expressed by Equation (26):

$$\min(x) = \pi \left(x_2^2 - x_1^2\right) x_3(x_5 + 1) p_m \tag{26}$$

where $x_1 = r_i$, $x_2 = r_o$, $x_3 = t$, $x_4 = F$, $x_5 = Z$, subject to:

$$g_1(x) = x_2 - x_1 - \Delta R \ge 0$$

$$g_2(x) = L_{max} - (Z+1)(t+\delta) \ge 0$$

$$g_3(x) = p_{max} - p_{rz} \ge 0$$

$$g_4(x) = p_{max} V_{sr,max} - p_{rz} V_{sr} \ge 0$$

Biomimetics **2025**, 10, 342 37 of 41

$$g_5(x) = V_{sr,max} - V_{sr} \ge 0$$

$$g_6(x) = M_h - sM_s \ge 0$$

$$g_7(x) = T \ge 0$$

$$g_8(x) = T_{max} - T \ge 0$$

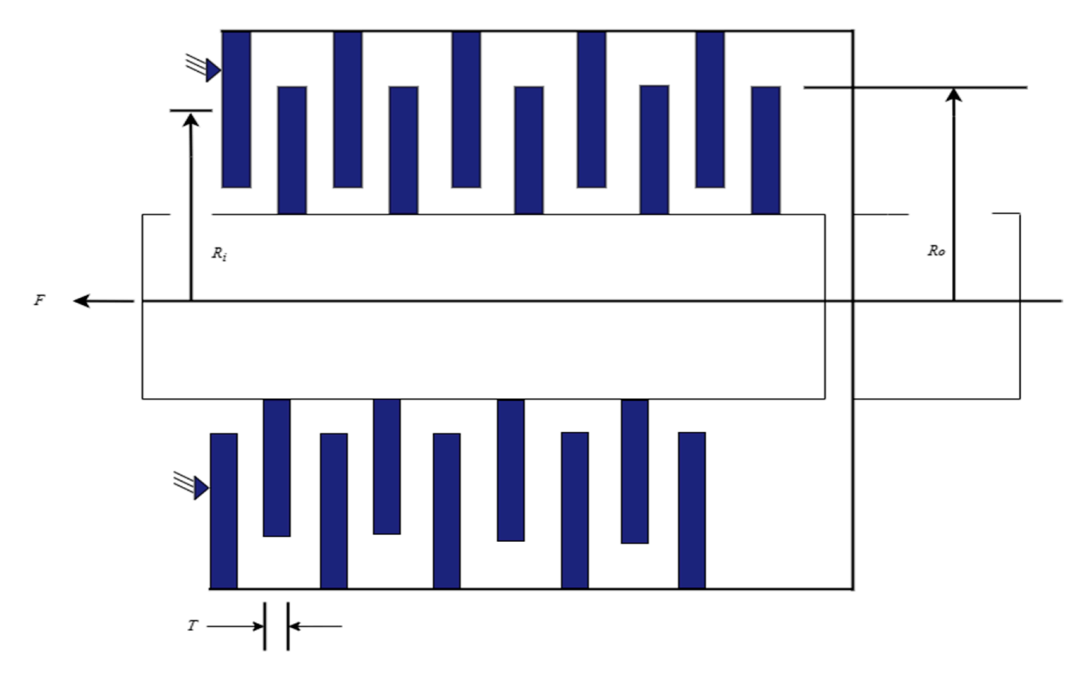


Figure 8. Schematic view of multiple-disk clutch brake design problem.

$$60 \le x_1 \le 80$$
 mm, $90 \le x_2 \le 110$ mm, $1.5 \le x_3 \le 3$ mm, $0 \le x_4 \le 1000$ N, $2 \le x_5 \le 9$ where:

$$\begin{split} p_m &= 0.0000078 \text{ kg/mm}^3, p_{max} = 1 \text{ MPa}, \mu = 0.5, V_{sr,max} = 10 \text{ m/s}, s = 1.5, T_{max} = 15 \text{ s}, \\ n &= 250 \text{ rpm}, M_f = 3 \text{ Nm}, I_z = 55 \text{kg/m}^2, \delta = 0.5 \text{ mm}, \Delta R = 20 \text{ mm}, L_{max} = 30 \text{ mm}, \\ M_h &= \frac{2}{3} \mu x_4 x_5 \frac{x_2^3 - x_1^3}{x_2^2 - x_1^2} \text{N mm}, w = \frac{\pi n}{30} \frac{\text{rad}}{\text{s}}, R_{\text{sr}} = \frac{2}{3} \frac{x_2^3 - x_1^3}{x_2^2 - x_1^2} \text{mm}, A = \pi \left(x_2^2 - x_1^2 \right) \text{mm}^2, \\ M_s &= 40 \text{ Nm}, p_{\text{rz}} = \frac{x_4}{\text{A}} \text{N/mm}^2, V_{\text{sr}} = \frac{\pi R_{\text{sr}} n}{30} \text{mm/s} \end{split}$$

Table 11 presents a comparison of the results for solving the multiple-disk clutch brake design problem using IVYPSO and other algorithms from the literature. The success rate threshold for this problem was determined to be 0.2352. The best result obtained by IVYPSO was $r_i=70$, $r_o=90$, t=1, F=1000, Z=2, with the lowest cost of 0.2352 and an SR value of 100%, and it required minimal time to complete the task. Table 12 shows a statistical analysis, showing that IVYPSO achieves the lowest average cost of 0.2352. These results indicate that compared to other optimization algorithms, IVYPSO provides a better solution for the multiple-disk clutch brake design problem.

Biomimetics **2025**, 10, 342 38 of 41

Table 11. The best values obtained by IVY	and other competing algorithms for the multiple-disk
clutch brake design problem.	

Algorithm	X1	X2	Х3	X4	X5	Optimal Value	SR (%)	ACTs	AFEs
IVYPSO	70	90	1	1000	2	0.2352	100	0.2261	15,030
PSO	70	90	1	1000	2	0.2352	90	0.2117	15,030
IVY	70	90	1	1000	2	0.2352	95	0.2644	15,030
BOA	69.7384	90	1.1944	405.0447	2	0.2842	0	0.3671	30,030
WOA	70	90	1	1000	2	0.2352	100	0.1843	15,000
GOOSE	70	90	1	1000	2	0.2352	90	0.2395	15,000
HPSOBOA	67.2176	91	0.8157	788.6999	1.8812	0.2731	0	0.6078	30,030
FDC_AGDE	70	90	1	1000	2	0.2352	100	0.2211	15,030
dFDB_LSHADE	69.9485	90	1	432.177	2	0.2358	0	0.0117	500
NSM_BO	70	90	1	1000	2	0.2352	100	0.4497	15,000
dFDB_SFS	70	90	1	1000	2	0.2352	85	0.3248	15,000
FDB_AGSK	70	90	1	1000	2	0.2352	100	0.2867	15,000

Note: The optimal values are highlighted in bold.

Table 12. Statistical assessment of various algorithms applied to the multiple-disk clutch brake design problem.

Algorithm	Mean	Best	Worst	Median	Std	Rank
IVYPSO	0.2352	0.2352	0.2352	0.2352	0	1
PSO	0.2381	0.2352	0.2638	0.2352	0.009	8
IVY	0.2354	0.2352	0.236	0.2352	0.0014	6
BOA	0.3149	0.2842	0.3308	0.3255	0.0234	11
WOA	0.2352	0.2352	0.2352	0.2352	0	1
GOOSE	0.2383	0.2352	0.2531	0.2352	0.006	9
HPSOBOA	0.3264	0.2731	0.3308	0.3308	0.0139	12
FDC_AGDE	0.2352	0.2352	0.2352	0.2352	0	1
dFDB_LSHADE	0.2376	0.2358	0.242	0.2371	0.002	7
NSM_BO	0.2352	0.2352	0.2352	0.2352	0	1
dFDB_SFS	0.2411	0.2352	0.2646	0.2352	0.0124	10
FDB_AGSK	0.2352	0.2352	0.2352	0.2352	0	1

Note: The optimal values are highlighted in bold.

6. Conclusions

The proposed IVYPSO algorithm effectively enhances both the global exploration and local exploitation capabilities within complex search spaces by integrating ivy growth variables and dynamic control factors into the classical PSO framework. The ivy growth variables facilitate diverse search behaviors that prevent premature convergence, while the dynamic control factors adaptively balance the emphasis between global and local searches based on fitness evaluations.

Extensive experiments on 26 benchmark functions and three challenging engineering optimization problems—including the multiple-disk clutch brake design and gas transmission compressor design—demonstrated that IVYPSO achieves superior solution quality with rapid convergence. Comparative analyses against ten state-of-the-art optimization algorithms further confirmed the algorithm's superiority in convergence accuracy, stability, and robustness, particularly in handling multi-modal and high-dimensional problems where the global optimization ability is critical.

This study lays a foundation for further research in several directions. Our future work will focus on extending IVYPSO to more complex engineering problems and multi-objective optimization scenarios, especially those involving dynamic, multi-modal, and high-dimensional environments. Moreover, the incorporation of adaptive parameter tuning strategies is planned to optimize the design of ivy growth variables and dynamic control factors, thereby improving the algorithm's flexibility and performance across diverse problem domains.

Biomimetics 2025, 10, 342 39 of 41

In addition, hybridizing IVYPSO with other intelligent optimization techniques, such as genetic algorithms, differential evolution, and simulated annealing, to build multifusion frameworks may offer significant performance enhancements. This would leverage complementary algorithmic strengths and further improve the solution quality and convergence behavior.

Author Contributions: Conceptualization, K.Z. and F.Y.; methodology, K.Z. and Y.J.; software, Y.J. and Z.Z.; validation, Y.J. and Z.Z.; formal analysis, F.Y.; investigation, K.Z. and Z.Z.; data curation, Y.J.; writing—original draft preparation, K.Z.; writing—review and editing, Z.M. and Y.P.; supervision, F.Y.; project administration, F.Y. All authors have read and agreed to the published version of the manuscript.

Funding: This research received no external funding.

Institutional Review Board Statement: Not applicable.

Informed Consent Statement: Not applicable.

Data Availability Statement: The datasets used and/or analyzed during the current study are publicly available and can be accessed without any restrictions. If needed, they can also be obtained by contacting the corresponding author.

Acknowledgments: This work was supported by equipment funded through the Intelligent Connected New Energy Vehicle Teaching System project of Chongqing University of Technology, under the national initiative "Promote Large-Scale Equipment Renewals and Trade-Ins of Consumer Goods".

Conflicts of Interest: The authors declare no conflict of interest. The authors declare that they have no known competing financial interests or personal relationships that could have appeared to influence the work reported in this paper.

References

- 1. Sattar, D.; Salim, R. A smart metaheuristic algorithm for solving engineering problems. *Eng. Comput.* **2021**, *37*, 2389–2417. [CrossRef]
- 2. Abualigah, L.; Elaziz, M.A.; Khasawneh, A.M.; Alshinwan, M.; Ibrahim, R.A.; Al-Qaness, M.A.A.; Mirjalili, S.; Sumari, P.; Gandomi, A.H. Meta-heuristic optimization algorithms for solving real-world mechanical engineering design problems: A comprehensive survey, applications, comparative analysis, and results. *Neural Comput. Appl.* 2022, 34, 4081–4110. [CrossRef]
- 3. Talbi, E.G. Machine learning into metaheuristics: A survey and taxonomy. ACM Comput. Surv. (CSUR) 2021, 54, 1–32. [CrossRef]
- 4. Kaveh, M.; Mesgari, M.S. Application of meta-heuristic algorithms for training neural networks and deep learning architectures: A comprehensive review. *Neural Process. Lett.* **2023**, *55*, 4519–4622. [CrossRef] [PubMed]
- 5. Katebi, J.; Shoaei-Parchin, M.; Shariati, M.; Trung, N.T.; Khorami, M. Developed comparative analysis of metaheuristic optimization algorithms for optimal active control of structures. *Eng. Comput.* **2020**, *36*, 1539–1558. [CrossRef]
- 6. Joseph, S.B.; Dada, E.G.; Abidemi, A.; Oyewola, D.O.; Khammas, B.M. Metaheuristic algorithms for PID controller parameters tuning: Review, approaches and open problems. *Heliyon* **2022**, *8*, e09399. [CrossRef]
- 7. Ahmadianfar, I.; Bozorg-Haddad, O.; Chu, X. Gradient-based optimizer: A new metaheuristic optimization algorithm. *Inf. Sci.* **2020**, *540*, 131–159. [CrossRef]
- 8. Abdel-Basset, M.; Mohamed, R.; Elkomy, O.M.; Abouhawwash, M. Recent metaheuristic algorithms with genetic operators for high-dimensional knapsack instances: A comparative study. *Comput. Ind. Eng.* **2022**, *166*, 107974. [CrossRef]
- 9. Keivanian, F.; Chiong, R. A novel hybrid fuzzy–metaheuristic approach for multimodal single and multi-objective optimization problems. *Expert Syst. Appl.* **2022**, *195*, 116199. [CrossRef]
- 10. Huang, Y.; Lu, S.; Liu, Q.; Han, T.; Li, T. GOHBA: Improved Honey Badger Algorithm for Global Optimization. *Biomimetics* **2025**, 10, 92. [CrossRef]
- 11. Zhu, X.; Zhang, J.; Jia, C.; Liu, Y.; Fu, M. A Hybrid Black-Winged Kite Algorithm with PSO and Differential Mutation for Superior Global Optimization and Engineering Applications. *Biomimetics* **2025**, *10*, 236. [CrossRef] [PubMed]
- 12. Choi, K.; Jang, D.-H.; Kang, S.-I.; Lee, J.-H.; Chung, T.-K.; Kim, H.-S. Hybrid algorithm combing genetic algorithm with evolution strategy for antenna design. *IEEE Trans. Magn.* **2015**, *52*, 7209004. [CrossRef]
- 13. Yu, X.; Jiang, N.; Wang, X.; Li, M. A hybrid algorithm based on grey wolf optimizer and differential evolution for UAV path planning. *Expert Syst. Appl.* **2023**, 215, 119327. [CrossRef]

Biomimetics **2025**, 10, 342 40 of 41

14. Peng, Y.; Wang, Y.; Hu, F.; He, M.; Mao, Z.; Huang, X.; Ding, J. Predictive modeling of flexible EHD pumps using Kolmogorov–Arnold Networks. *Biomim. Intell. Robot.* **2024**, *4*, 100184. [CrossRef]

- 15. Mao, Z.; Bai, X.; Peng, Y.; Shen, Y. Design, modeling, and characteristics of ring-shaped robot actuated by functional fluid. *J. Intell. Mater. Syst. Struct.* **2024**, *35*, 1459–1470. [CrossRef]
- 16. Kennedy, J.; Eberhart, R. Particle swarm optimization. In Proceedings of the ICNN'95-International Conference on Neural Networks, Perth, Australia, 27 November–1 December 1995; IEEE: Piscataway, NJ, USA, 1995; Volume 4, pp. 1942–1948.
- 17. Papazoglou, G.; Biskas, P. Review and comparison of genetic algorithm and particle swarm optimization in the optimal power flow problem. *Energies* **2023**, *16*, 1152. [CrossRef]
- 18. Thangaraj, R.; Pant, M.; Abraham, A.; Bouvry, P. Particle swarm optimization: Hybridization perspectives and experimental illustrations. *Appl. Math. Comput.* **2011**, 217, 5208–5226. [CrossRef]
- 19. Sun, J.; Xu, W.; Feng, B. Adaptive parameter control for quantum-behaved particle swarm optimization on individual level. In Proceedings of the 2005 IEEE International Conference on Systems, Man and Cybernetics, Waikoloa, HI, USA, 12 October 2015; IEEE: Piscataway, NJ, USA, 2005; Volume 4, pp. 3049–3054.
- 20. Song, Y.; Liu, Y.; Chen, H.; Deng, W. A multi-strategy adaptive particle swarm optimization algorithm for solving optimization problem. *Electronics* **2023**, *12*, 491. [CrossRef]
- 21. Ghasemi, M.; Zare, M.; Trojovský, P.; Rao, R.V.; Trojovská, E.; Kandasamy, V. Optimization based on the smart behavior of plants with its engineering applications: Ivy algorithm. *Knowl. Based Syst.* **2024**, 295, 111850. [CrossRef]
- 22. Kahraman, H.T.; Aras, S.; Gedikli, E. Fitness-distance balance (FDB): A new selection method for meta-heuristic search algorithms. Knowl. Based Syst. 2020, 190, 105169. [CrossRef]
- 23. Duman, S.; Kahraman, H.T.; Kati, M. Economical operation of modern power grids incorporating uncertainties of renewable energy sources and load demand using the adaptive fitness-distance balance-based stochastic fractal search algorithm. *Eng. Appl. Artif. Intell.* 2023, 117, 105501. [CrossRef]
- 24. Kahraman, H.T.; Bakir, H.; Duman, S.; Katı, M.; Aras, S.; Guvenc, U. Dynamic FDB selection method and its application: Modeling and optimizing of directional overcurrent relays coordination. *Appl. Intell.* **2022**, *52*, 4873–4908. [CrossRef]
- 25. Ozkaya, B.; Kahraman, H.T.; Duman, S.; Guvenc, U. Fitness-Distance-Constraint (FDC) based guide selection method for constrained optimization problems. *Appl. Soft Comput.* **2023**, *144*, 110479. [CrossRef]
- 26. Yildirim, I.; Bozkurt, M.H.; Kahraman, H.T.; Aras, S. Dental X-Ray image enhancement using a novel evolutionary optimization algorithm. *Eng. Appl. Artif. Intell.* **2025**, 142, 109879. [CrossRef]
- 27. Kahraman, H.T.; Hassan, M.H.; Katı, M.; Tostado-Véliz, M.; Duman, S.; Kamel, S. Dynamic-fitness-distance-balance stochastic fractal search (dFDB-SFS algorithm): An effective metaheuristic for global optimization and accurate photovoltaic modeling. *Soft Comput.* 2024, 28, 6447–6474. [CrossRef]
- 28. Bakır, H.; Duman, S.; Guvenc, U.; Kahraman, H.T. Improved adaptive gaining-sharing knowledge algorithm with FDB-based guiding mechanism for optimization of optimal reactive power flow problem. *Electr. Eng.* **2023**, *105*, 3121–3160. [CrossRef]
- 29. Hamad, R.K.; Rashid, T.A. GOOSE algorithm: A powerful optimization tool for real-world engineering challenges and beyond. *Evol. Syst.* **2024**, *15*, 1249–1274. [CrossRef]
- 30. Zhang, M.; Long, D.; Qin, T.; Yang, J. A chaotic hybrid butterfly optimization algorithm with particle swarm optimization for high-dimensional optimization problems. *Symmetry* **2020**, *12*, 1800. [CrossRef]
- 31. Kahraman, H.T.; Katı, M.; Aras, S.; Taşci, D.A. Development of the Natural Survivor Method (NSM) for designing an updating mechanism in metaheuristic search algorithms. *Eng. Appl. Artif. Intell.* **2023**, 122, 106121. [CrossRef]
- 32. Öztürk, H.T.; Kahraman, H.T. Metaheuristic search algorithms in Frequency Constrained Truss Problems: Four improved evolutionary algorithms, optimal solutions and stability analysis. *Appl. Soft Comput.* **2025**, 171, 112854. [CrossRef]
- 33. Ouyang, H.; Li, W.; Gao, F.; Huang, K.; Xiao, P. Research on Fault Diagnosis of Ship Diesel Generator System Based on IVY-RF. *Energies* **2024**, *17*, 5799. [CrossRef]
- 34. Jamil, M.; Yang, X.S. A literature survey of benchmark functions for global optimisation problems. *Int. J. Math. Model. Numer. Optim.* **2013**, *4*, 150–194. [CrossRef]
- 35. Zhan, Z.-H.; Shi, L.; Tan, K.C.; Zhang, J. A survey on evolutionary computation for complex continuous optimization. *Artif. Intell. Rev.* **2022**, *55*, 59–110. [CrossRef]
- 36. Cai, T.; Zhang, S.; Ye, Z.; Zhou, W.; Wang, M.; He, Q.; Chen, Z.; Bai, W. Cooperative metaheuristic algorithm for global optimization and engineering problems inspired by heterosis theory. *Sci. Rep.* **2024**, *14*, 28876. [CrossRef]
- 37. Mao, Z.; Hosoya, N.; Maeda, S. Flexible electrohydrodynamic fluid-driven valveless water pump via immiscible interface. *Cyborg Bionic Syst.* **2024**, *5*, 0091. [CrossRef]
- 38. Lau, S.L.H.; Lim, J.; Chong, E.K.P.; Wang, X. Single-pixel image reconstruction based on block compressive sensing and convolutional neural network. *Int. J. Hydromechatronics* **2023**, *6*, 258–273. [CrossRef]
- 39. Verma, H.; Siruvuri, S.V.; Budarapu, P.R. A machine learning-based image classification of silicon solar cells. *Int. J. Hydromechatronics* **2024**, 7, 49–66. [CrossRef]

Biomimetics **2025**, 10, 342 41 of 41

40. Alawi, O.A.; Kamar, H.M.; Shawkat, M.M.; Al Ani, M.M.; Mohammed, H.A.; Homod, R.Z.; Wahid, M.A. Artificial intelligence-based viscosity prediction of polyalphaolefin-boron nitride nanofluids. *Int. J. Hydromechatro.* **2024**, *7*, 89–112. [CrossRef]

- 41. Arora, S.; Singh, S. Butterfly optimization algorithm: A novel approach for global optimization. *Soft Comput.* **2019**, 23, 715–734. [CrossRef]
- 42. Mirjalili, S.; Lewis, A. The whale optimization algorithm. Adv. Eng. Softw. 2016, 95, 51–67. [CrossRef]
- 43. Yuan, F.; Huang, X.; Zheng, L.; Wang, Y.; Yan, X.; Gu, S.; Peng, Y. The Evolution and Optimization Strategies of a PBFT Consensus Algorithm for Consortium Blockchains. *Information* **2025**, *16*, 268. [CrossRef]
- 44. Zhang, C.; Chen, J.; Li, J.; Peng, Y.; Mao, Z. Large language models for human–robot interaction: A review. *Biomim. Intell. Robot.* **2023**, *3*, 100131. [CrossRef]
- 45. Peng, Y.; Yang, X.; Li, D.; Ma, Z.; Liu, Z.; Bai, X.; Mao, Z. Predicting flow status of a flexible rectifier using cognitive computing. *Expert Syst. Appl.* **2025**, 264, 125878. [CrossRef]
- 46. Bai, X.; Peng, Y.; Li, D.; Liu, Z.; Mao, Z. Novel soft robotic finger model driven by electrohydrodynamic (EHD) pump. *J. Zhejiang Univ. Sci. A* **2024**, 25, 596–604. [CrossRef]
- 47. Mao, Z.; Peng, Y.; Hu, C.; Ding, R.; Yamada, Y.; Maeda, S. Soft computing-based predictive modeling of flexible electrohydrodynamic pumps. *Biomim. Intell. Robot.* **2023**, *3*, 100114. [CrossRef]
- 48. Peng, Y.; Sakai, Y.; Funabora, Y.; Yokoe, K.; Aoyama, T.; Doki, S. Funabot-Sleeve: A Wearable Device Employing McKibben Artificial Muscles for Haptic Sensation in the Forearm. *IEEE Robot. Autom. Lett.* **2025**, *10*, 1944–1951. [CrossRef]
- 49. Mao, Z.; Kobayashi, R.; Nabae, H.; Suzumori, K. Multimodal strain sensing system for shape recognition of tensegrity structures by combining traditional regression and deep learning approaches. *IEEE Robot. Autom. Lett.* **2024**, *9*, 10050–10056. [CrossRef]
- Dai, L.; Zhang, L.; Chen, Z. GrS Algorithm for Solving Gas Transmission Compressor Design Problem. In Proceedings of the 2022 IEEE/WIC/ACM International Joint Conference on Web Intelligence and Intelligent Agent Technology (WI-IAT), Niagara Falls, ON, Canada, 17–20 November 2022; IEEE: Piscataway, NJ, USA, 2022; pp. 842–846.
- 51. Dhiman, G.; Kaur, A. Spotted hyena optimizer for solving engineering design problems. In Proceedings of the 2017 International Conference on Machine Learning and Data Science (MLDS), Noida, India, 14–15 December 2017; IEEE: Piscataway, NJ, USA, 2017; pp. 114–119.

Disclaimer/Publisher's Note: The statements, opinions and data contained in all publications are solely those of the individual author(s) and contributor(s) and not of MDPI and/or the editor(s). MDPI and/or the editor(s) disclaim responsibility for any injury to people or property resulting from any ideas, methods, instructions or products referred to in the content.